Charge-exchange reactions with lithium ions and their use in the study of nuclear structure

F. A. Gareev and S. N. Ershov

Joint Institute for Nuclear Research, Dubna

A. A. Ogloblin and S. B. Sakuta

I. V. Kurchatov Institute of Atomic Energy, Moscow

Fiz. Elem. Chastits At. Yadra **20**, 1293–1340 (November–December 1989)

Charge-exchange reactions, which are currently the most universal means of study of isobaric transitions, are reviewed. The main attention is paid to experiments made recently with beams of ^{6}Li and ^{7}Li ions at energies higher than 10 MeV/nucleon at the cyclotron of the I. V. Kurchatov Institute of Atomic Energy and with other cyclotrons in the world. The importance of the one-step charge-exchange mechanism in the (^{6}Li, ^{6}He) and (^{7}Li, ^{7}Be) processes is demonstrated. Specific examples of the use of these reactions for the study of the spin–isospin structure of nuclei are considered. A comparison is made with other charge-exchange reactions induced by both light and heavier ions. The results of (^{6}Li, ^{6}He) experiments to investigate precritical effects are analyzed, and the radial dependence of the form factor of the quasielastic process at short distances is also considered.

INTRODUCTION

Charge-exchange reactions are nuclear processes in which a neutron of a target nucleus is transformed into a proton or vice versa. They are the most universal means of study of isobaric transitions, since they permit investigations in the complete region of excitation of nuclei, including the region that is inaccessible for β decay. Indeed, it was in these reactions that isobar analog states were discovered already at the beginning of the Sixties. These states take up all the strength of the single-particle transitions that take place without change of the orbital angular momentum and spin ($\Delta L = 0$, $\Delta S = 0$) and correspond in the language of β-decay theory to transitions of Fermi type. In recent years the interest in charge-exchange reactions has grown tremendously in connection with the discovery at the beginning of the Eighties of a new giant isobaric resonance corresponding to Gamow–Teller transitions ($\Delta L = 0$, $\Delta S = 1$). Both of the monopole isobaric resonances were discovered in the (p, n) reaction—the first at proton energies 10–20 MeV,[1] and the second at energies 100–200 MeV.[2] This success was due not only to the fact that the (p, n) reaction has a unique kinematic selectivity with respect to $\Delta L = 0$ transitions but also to its dynamical properties, namely, the dominance of Fermi transitions at low proton energies and of Gamow–Teller transitions at high energies.

Experiments with protons also showed that the charge-exchange excitations are not exhausted by monopole transitions and that multipole isobaric resonances ($\Delta L > 0$) are also possible.[3] However, in this case the (p, n) reaction completely loses its advantages over other charge-exchange reactions in which heavier incident particles are used. The reason for this is that the differential cross sections for $\Delta L \geqslant 1$ transitions decrease so strongly that the result depends strongly on the manner in which the background is subtracted. In this case, charge-exchange reactions in which complex particles participate may be preferable, first because the kinematic selectivity with respect to $\Delta L \geqslant 1$ transitions increases and, second, because the physical background associated with processes that differ from the direct charge-exchange mechanism, for example, knockout, pre-equilibrium emission, and many-step processes, can be much smaller.

The extent to which the direct charge-exchange mechanism will dominate over the other mechanisms also depends on the extent to which the wave functions of the incident and emitted particles overlap. Let us consider from this point of view various reactions in which complex particles participate. Table I gives possible charge-exchange reactions in which a proton of the incident particle is transformed into a neutron. Table II gives examples of the inverse reactions with the transformation of a neutron into a proton. A measure of the overlap of the wave functions of the ground states of the initial and final particles is $\log ft$, which can be determined from β-decay experiments and is related to the transition matrix element M_{if} ($K/ft = M_{if}^2$).

It can be seen from Table I that ^{6}He and ^{6}Li have structures that are most nearly identical; between them a superallowed Gamow–Teller transition with a record value of $\log ft$ is realized. For example, the square of the matrix element of the ^{6}He–^{6}Li transition is two times and an order of magnitude greater than the corresponding quantities for the n–p and ^{12}B–^{12}C transitions.

With regard to reactions with transformation of a neutron into a proton in the incident particle (Table II), the most promising reaction for the study of isobaric transitions is the (^{7}Li, ^{7}Be) reaction. Although $\log ft$ for the ^{7}Be–^{7}Li transition is somewhat greater than for n–p and t–^{3}He, beams of ^{7}Li ions do not now present a severe technical problem compared with the difficulties that arise in the preparation of monoenergetic and intense high-energy beams of neutrons and radioactive tritium.

When choosing a specific charge-exchange reaction for the study of charge-exchange excitations one must also bear in mind how many stable states the emitted particle possesses. In this respect lithium ions also are generally advantageous compared with heavier ions (see Tables I and II).

These are the reasons why the present review is devoted to charge-exchange reactions with lithium ions. We begin by considering properties of charge-exchange reactions and general relations for calculating differential cross sections

 0090-4759/89/060541-28$04.40

TABLE I. Charge-exchange reactions of (p, n) type.

a	J^π	b	J^π	lg ft	Type of decay	Number of bound states
p	$1/2^+$	n	$1/2^+$	3.07	$F+GT$	1
^{3}He	$1/2^+$	^{3}H	$1/2^+$	3.03	$F+GT$	1
^{6}Li	1^+	^{6}He	0^+	2.8	GT	1
^{9}Be	$3/2^-$	^{9}Li	$3/2^-$	5.31	$F+GT$	2
^{10}B	3^+	^{10}Be	0^+	13.42	GT *	6
^{11}B	$3/2^-$	^{11}Be	$1/2^+$	6.83	F*$+GT$**	2
^{12}C	0^+	^{12}B	1^+	4.067	GT	5
^{13}C	$1/2^-$	^{13}B	$3/2^-$	4.01	GT	7
^{14}N	1^+	^{14}C	0^+	9.04	GT	7
^{16}O	0^+	^{16}N	2^-	9.1	GT **	4

*Transitions forbidden in the second order.
**Transitions forbidden in the first order.

when the incident particles are ^{6}Li and ^{7}Li. Section 2 contains the main results of the experimental investigation of charge-exchange reactions obtained using beams of the light particles p, n, d, and ^{3}He. These results are needed for better understanding of the position occupied by heavy ions in the general problem of the charge-exchange excitations of nuclei. The following sections present the results of investigations of the mechanism of the (^{6}Li, ^{6}He) and (^{7}Li, ^{7}Be) reactions and of their use in the study of spin–isospin structure of nuclei. The final section is devoted to applications of the (^{6}Li, ^{6}He) reaction. Two experiments are discussed. The first is associated with the search for manifestations of the proximity of nuclei to the threshold of π-condensate instability. The second is associated with the determination of the form factor of the quasielastic process at short distances.

1. GENERAL PROPERTIES OF CHARGE-EXCHANGE REACTIONS

A characteristic and important feature of charge-exchange reactions is that through them isovector excitation modes can be studied separately from isoscalar modes. This cannot be done, for example, in inelastic scattering of protons and electrons.

In the general case, when the target nucleus has isospin $T_0[T_Z = (N-Z)/2]$, isovector transitions lead to three types of states characterized by isospins—$T_0 - 1$, T_0, and $T_0 + 1$ (Fig. 1). They are all excited in charge-exchange reactions in the direction of a decrease of the projection of the isospin ($\Delta T_Z = -1$). Inelastic scattering ($\Delta T_Z = 0$) gives two states: T_0 and $T_0 + 1$. Even greater selectivity is achieved in the other branch of charge-exchange excitations proceeding in the direction of increasing projection of the isospin ($\Delta T_Z = +1$). In this case only transitions to states with $T = T_0 + 1$ are possible.

The strength of isovector transitions to different T states in charge-exchange reactions and in inelastic scattering can be gauged from the isospin Clebsch–Gordan coefficients, which are given in Table III. Under otherwise identical conditions, the transition cross sections will be proportional to the squares of these quantities. Therefore, for nuclei with a sufficiently large neutron, excess reactions of the (p, n) type will predominantly populate states with $T = T_0 - 1$, while inelastic scattering will populate states with T_0.

The reaction mechanism imposes certain restrictions on the spins and parities of the final states of the nuclei. If a reaction is realized by one-step charge exchange, then in the case of complex projectile nuclei we have the following selection rules:

$$J_t = L_t + S, \ \Delta\pi = (-1)^{L_t};$$
$$J_p = L_p + S, \ \Delta\pi = (-1)^{L_p},$$

where the subscript t identifies the system of the target nucleus and the product nucleus, while the subscript p identifies the system of the projectile nucleus and the emitted particle; J, L, and S are the total angular-momentum transfer, the orbital angular-momentum transfer, and the spin transfer. For charge exchange without spin flip $S = 0$, and with spin flip $S = 1$.

If ^{6}Li nuclei are used as projectiles and ^{6}He is detected, then, as was first noted in Refs. 4 and 5, only the value $S = 1$ is allowed, since the ground states of the ^{6}Li and ^{6}He nuclei are characterized by quantum numbers (LST) equal to

TABLE II. Charge-exchange reactions of (n, p) type.

a	J^π	b	J^π	lg ft	Type of decay	Number of bound states
n	$1/2^+$	p	$1/2^+$	3.07	$F+GT$	1
^{3}H	$1/2^+$	^{3}He	$1/2^+$	3.03	$F+GT$	1
^{7}Li	$3/2^-$	^{7}Be	$3/2^-$	3.32	$F+GT$	2
^{11}B	$3/2^-$	^{11}C	$3/2^-$	3.599	$F+GT$	8
^{12}C	0^+	^{12}N	1^+	4.12	GT	1
^{13}C	$1/2^-$	^{13}N	$1/2^-$	3.667	$F+GT$	1
^{14}N	1^+	^{14}O	0^+	7.266	GT	1
^{18}O	0^+	^{18}F	1^+	3.554	GT	18

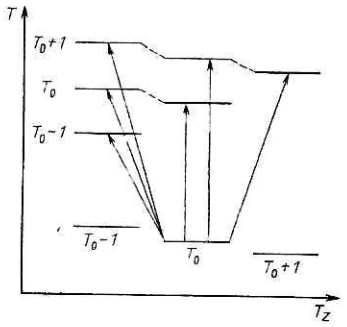

FIG. 1. Scheme of isovector transitions in charge-exchange reactions and in inelastic scattering.

(010) and (001), respectively. This means that transitions to the final states of the nuclei must be induced exclusively by the spin–isospin term in the central part of the nucleon–nucleon interaction potential. For $S=1$, the $0^+ \to 0^+$ transitions are strictly forbidden, and there will also be strong suppression of excitations of particle–hole states of normal parity constructed on "diagonal" (jl–jl) configurations. It is also readily seen that anomalous-parity states can be exicted only with spin flip, while normal-parity states can be excited with both $S=0$ and $S=1$.

For the (^{7}Li, ^{7}Be) reaction the selection rules do not give the selectivity with respect to S that occurs in the (^{6}Li, ^{6}He) case. However, as we have already noted, it has undoubted methodological advantages over the analogous (n, p) and (t, ^{3}He) reactions.

2. CALCULATION OF DIFFERENTIAL CROSS SECTIONS FOR THE DIRECT CHARGE-EXCHANGE PROCESS

General relations

In the distorted-wave method, the amplitude T_{if} of the reaction $A(a, b)B$ is expressed in the form

$$T_{if} = \int \psi_f^{(-)*}(\mathbf{k}_f, \mathbf{r})\, F(\mathbf{r})\, \psi_i^{(+)}(\mathbf{k}_i, \mathbf{r})\, dr, \qquad (1)$$

where $\psi_{i(f)}$ are the distorted waves that describe the relative motion of the nuclei in the entrance (respectively, exit) channel, and $F(r)$ is the reaction form factor:

$$F(\mathbf{r}) = \sum_{pt} \langle Bb \mid V_{pt} \mid Aa \rangle. \qquad (2)$$

Here, B, b and A, a are the internal wave functions of the nuclei that participate in the reaction, and the subscripts t and p label the "active" particles of the target nucleus and the incident particle, respectively.

Restricting ourselves to just the central and tensor components, we can express the interaction responsible for the charge exchange in the general form

$$V_{pt} = \{V_\tau^C(r_{pt}) + V_{\sigma\tau}^C(r_{pt})\, \boldsymbol{\sigma}_p \boldsymbol{\sigma}_t + V_\tau^T(r_{pt})\, S_{pt}\}\, \boldsymbol{\tau}_p \boldsymbol{\tau}_t, \qquad (3)$$

where $\boldsymbol{\sigma}$ and $\boldsymbol{\tau}$ are spin and isospin Pauli operators; $S_{pt} = 3(\boldsymbol{\sigma}_p \cdot \hat{r}_{pt})(\boldsymbol{\sigma}_t \hat{r}_{pt}) - \boldsymbol{\sigma}_p \boldsymbol{\sigma}_t$; $V_\tau^C(r_{pt})$, $V_{\sigma\tau}^C(r_{pt})$, $V_\tau^T(r_{pt})$ determine the radial dependence of the central (C) and tensor (T) interactions with respect to the distance $r_{pt} = |\mathbf{r} + \mathbf{r}_p - \mathbf{r}_t|$ between the nucleons, where, r is the distance between the centers of mass of the colliding nuclei, and $\mathbf{r}_p$ and $\mathbf{r}_t$ are, respectively, the coordinates of the p and t nucleon with respect to the center of mass of the nucleus a (respectively, A).

One generally uses the Gaussian form

$$V(r) = V \exp(-\alpha_G^2 r^2), \quad \alpha_G^{-1} = 1.8\ \text{F} \qquad (4)$$

or a superposition of Yukawa potentials with a term $\delta(r)$ to imitate exchange effects,[6]

$$V(r) = \sum_{i=1}^{3} a_i \exp(-b_i r)/b_i r + c\delta(r), \qquad (5)$$

and the form factors $F(r)$, which contain all information about the properties of the nuclei, can be expanded with respect to partial waves:

$$F(r) = \sum_{L_r M_r J_p M_p J_t M_t} \times (J_A M_A J_t M_t \mid J_B M_B)(J_b M_b J_p M_p \mid J_a M_a) \times (L_r M_r J_p M_p \mid J_t M_t)\, i^{-L_r} Y_{L_r M_r}^*(\Omega_r)\, \mathcal{F}^{L_r J_p J_t}(r). \qquad (6)$$

For this it is convenient to use a Fourier–Bessel transformation of the radial part of the interaction:

$$V(r_{pt}) = (2\pi)^{-3} \int d\mathbf{k}\, \tilde{V}(\mathbf{k})\, e^{i\mathbf{k}\mathbf{r}_{pt}}; \qquad (7)$$

$$\tilde{V}(\mathbf{k}) = 4\pi \int V(r_{pt})\, j_0(kr_{pt})\, r_{pt}^2\, dr_{pt}. \qquad (8)$$

Then, taking into account only the central components of the interaction for the radial part of the form factor, we obtain the expression[7,8]

TABLE III. Clebsch–Gordan isospin coefficients.

T \ T_z	T_0-1 (p, n)	T_0 (p, p')	T_0+1 (n, p)
T_0+1	$\sqrt{\frac{1}{(2T_0+1)(T_0+1)}}$	$\sqrt{\frac{1}{T_0+1}}$	1
T_0	$\sqrt{\frac{1}{T_0+1}}$	$\sqrt{\frac{T_0}{T_0+1}}$	—
T_0-1	$\sqrt{\frac{2T_0-1}{2T_0+1}}$	—	—

$$\mathcal{F}^{L_r J_p J_t}(r) = \sum_{TM_T SL_p L_t} G_{ST}(-1)^{J_a - J_b + T_b - T_a} \times \hat{T}_a^{-1}\hat{T}_B^{-1}\hat{J}_a^{-1}\hat{J}_B^{-1}\hat{J}_p\hat{L}_p\hat{L}_t(T_A M_A T M_T \mid T_B M_B) \times (T_b M_b T M_T \mid T_a M_a) \times (L_p 0 L_t 0 \mid L_r 0) W(J_p L_p J_t L_t, SL_r) I_{ST}(r), \quad (9)$$

where $\hat{x} \equiv (2x+1)^{1/2}$, $G_{01} = V_\tau$, $G_{11} = V_{\sigma\tau}$,

$$I_{ST}(r) = \frac{1}{4(\pi)^{5/2}} \int_0^\infty dk k^2 j_{L_r}(kr) \tilde{\rho}_{ab}^{L_p S J_p, T}(k) \tilde{\rho}_{AB}^{L_t S J_t, T}(k) \tilde{V}(k); \quad (10)$$

$$\tilde{\rho}_{ab}^{L_p S J_p, T}(k) = 4\pi \int_0^\infty dr_p r_p^2 j_{L_p}(kr_p) \rho_{ab}^{L_p S J_p, T}(r_p); \quad (11)$$

$$\tilde{\rho}_{AB}^{L_t S J_t, T}(k) = 4\pi \int_0^\infty dr r_t^2 j_{L_t}(kr_t) \rho_{AB}^{L_t S J_t, T}(r_t). \quad (12)$$

The transition densities ρ_{ab} and ρ_{AB} refer to the "light" and "heavy" systems, respectively, and their actual form also depends on the chosen nuclear model and is determined in the standard manner:

$$\rho_{ab}^{L_p S J_p, T}(r_p) = \langle J_b T_b \| \sum \frac{\delta(r_p - r_p')}{r_p'^2} T^{L_p S J_p} \times (p') \tau^T(p') \| J_a T_a \rangle; \quad (13)$$

$$T_M^{LSJ}(e) \equiv i^L [Y_L(\Omega_e) \times \sigma^S(e)]_M^J. \quad (14)$$

Here, J_p and J_t are the total angular momenta transferred in the process of the reaction to the incident ion and to the target nucleus, and L_r is the change in the angular momentum of the relative motion of the colliding nuclei.

From (6) and (9) we obtain the selection rules

$$\Delta(T_a T T_b), \ \Delta(T_A T T_B);$$
$$\Delta(J_a J_p J_b), \ \Delta(L_p S J_p), \ \Delta\pi_{ab} = (-1)^{L_p};$$
$$\Delta(J_A J_t J_B), \ \Delta(L_t S J_t), \ \Delta\pi_{AB} = (-1)^{L_t};$$
$$\Delta(J_p J_t L_r), \ \Delta(L_p L_t L_r), \ \Delta\pi_{ab} \cdot \Delta\pi_{AB} = (-1)^{L_r}.$$

Details of calculations for the (^{6}Li, ^{6}He) reaction

Since the ^{6}Li and ^{6}He nuclei are "fragile" systems, the (^{6}Li, ^{6}He) reaction has a surface nature. Therefore, the wave functions of these nuclei, and also of the target nucleus and the product nucleus, must be calculated with sufficiently good accuracy at large distances. In this paper, we use shell wave functions for the target nucleus and product nucleus, corrected at large distances by means of the well-depth prescription (WDP), the ^{6}Li and ^{6}He wave functions obtained in the framework of the three-particle $\alpha + N + N$ model being used. In accordance with Refs. 9 and 10, the ^{6}Li and ^{6}He wave functions can be expressed in the LS-coupling scheme in the form

$$\psi_i^{JM}(x_i y_i \sigma_{N_1} \sigma_{N_2}) = \psi_\alpha(1) \sum_{LSM_L M_S} (LM_L SM_S \mid JM) \psi^{SM_S}(\sigma_{N_1}\sigma_{N_2}) \times \sum_{\lambda_i l_i \mu_i m_i} (\lambda_i \mu_i l_i m_i \mid LM_L) Y_{\lambda_i \mu_i}(\hat{x}_i) Y_{l_i m_i}(\hat{y}) \Phi_{\lambda_i l_i}^L(x_i y_i), \quad (15)$$

where $Y_{\lambda\mu}(\hat{x}_i)$, $Y_{lm}(\hat{y}_i)$ and $\psi^{SM_S}(\sigma_{N_1}\sigma_{N_2})$ are spherical and spin functions, respectively, $\Phi_{\lambda l}^L(x, y)$ is the radial part of the wave function, and ψ_α is the α-particle wave function. As a consequence of the method chosen to describe the ^{6}Li and ^{6}He nuclei, the nucleons of the α-particle core do not participate in the reaction. In what follows, we shall use the coordinate system illustrated in Fig. 2. Then

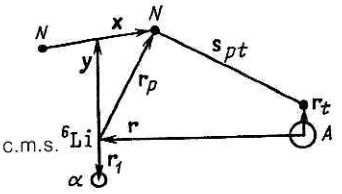

FIG. 2. Coordinate system for the (^{6}Li, ^{6}He) reaction.

$$\mathbf{S}_{pt} = \mathbf{r} + \mathbf{r}_p - \mathbf{r}_t = a_p \mathbf{x} + b_p \mathbf{y} + \mathbf{r} - \mathbf{r}_t, \quad (16)$$

where the coefficients a_p and b_p are determined in Refs. 9 and 10. As can be seen from Fig. 2, we take into account the recoil effects for the light system ^{6}Li or ^{6}He, which in many cases are very important.[12] Allowance for the three-body aspects of the problem has the consequence that the form factor $F(r)$ (2) contains nine-dimensional integrals, and not six-dimensional integrals, as was the case in the approximations of Refs. 7 and 11.

The radial part of the function (15) was expanded[10] with respect to a basis set of functions of Gaussian type:

$$\Phi_{\lambda l}^L(x_i y_i) = \sum_j C_j N_j x_i^\lambda y_i^l \exp\{-\alpha_{\lambda j} x_i^2 - \beta_{l_i} y_i^2\}. \quad (17)$$

Such a representation of the radial functions makes it possible to integrate with respect to the coordinates x and y explicitly and to obtain a simple integral with respect to the coordinate r_t.

Details of calculations for the (^{7}Li, ^{7}Be) reaction

We assume that the ^{7}Li and ^{7}Be nuclei consist of two clusters: an α particle and a three-nucleon nucleus (^{3}H or ^{3}He). Both clusters are in their ground states, and the α particle is treated as an inert structureless core that does not participate in the charge-exchange process. Then the wave function of the nuclei with $A = 7$ can be expressed in the form

$$\psi_{TN}^{JM_J} = \psi_\alpha(1) \sum_{lm\mu} \left(lm\tfrac{1}{2}\mu \mid JM_J\right) \times Y_{lm}(\Omega_R) \Phi_l(R) \psi_{TN}^{\frac{1}{2}\mu}(2, 3, 4), \quad (18)$$

where $\psi_\alpha(1)$ and $\psi_{TN}^{1/2\mu}(2, 3, 4)$ are the wave functions of the α particle and the nuclei with $A = 3$, respectively, and $\Phi_l(R)$ is the radial part of the wave function of the relative motion of the clusters with the given angular momentum l. The employed coordinate system is shown in Fig. 3, from which we see that

$$\mathbf{r}_p = a_p \boldsymbol{\chi}_4 + b_p \boldsymbol{\eta}_4 + c_p \mathbf{R} \ (p = 1, 2, 3, 4). \quad (19)$$

The coefficients a_p, b_p, and c_p are given in Ref. 13. The wave functions of the nuclei with $A = 3$ are taken from Ref. 14 in the LS-coupling scheme, and the radial part $\Phi_l(R)$ of the wave function of the relative motion of the clusters was expanded with respect to Gaussian functions[15]:

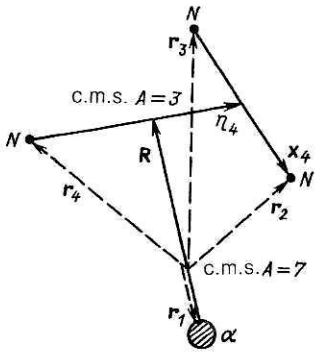

FIG. 3. Coordinate system for the (^{7}Li, ^{7}Be) reaction.

$$\Phi_l(R) = \sum_n C_n R^l \exp(-\alpha_n R^2). \quad (20)$$

The details of the calculation of the form factors can be found in Ref. 13; here we merely note that in the considered model $l_a = l_b = 1$, and therefore $L_p = 0, 2$, since $\Delta(l_a l_p l_b)$ and $\Delta\pi = (-1)^{l_a + l_b + L_p} = 1$.

3. CHARGE-EXCHANGE REACTIONS WITH LIGHT NUCLEI

The (p, n) reactions as a means of study of monopole isobaric transitions

The (p, n) reaction is ideal for the study of monopole isobaric transitions. By making a measurement at angle 0°, one can ensure conditions of maximal similarity between the charge-exchange process and β decay, in which the neutron is transformed into a proton essentially with zero momentum transfer. In charge exchange at angle 0°, the momentum transfer is determined by the well-known expression

$$q = 0.11Q/\sqrt{E_p}\ \text{F}^{-1}, \quad (21)$$

where Q is the reaction energy, and E_p (MeV) is the energy of the protons. Thus, the most favorable conditions for observing monopole transitions, and also maximal similarity with β decay, are obtained when the proton energy is higher. In this case, it is natural to expect the differential cross sections of the reaction to be proportional to the squares of the β-decay matrix elements, and, therefore, through this reaction the strength of the β transitions can also be readily measured in the region that is energetically inaccessible for β decay.

In the distorted-wave impulse approximation (DWIA), the dependence of the cross section of monopole transitions of the (p, n) reaction on the proton energy (E_p), the target mass (A), the momentum transfer (q), the change in the energy $\omega = E_x - Q_{g.s}$, and the structure of the initial and final states of the nuclei can be expressed[16] in terms of a product of three factors:

$$\sigma(q, \omega) = \hat{\sigma}_\alpha(E_p A)\, F(q\omega)\, B(\alpha), \quad (22)$$

where the subscript α characterizes the Fermi (F) or Gamow–Teller (GT) transition type. The first factor is a "reference" cross section $\hat{\sigma}(E_p, A)$ corresponding to unit transition strength in the limit $q = 0$, $\omega = 0$:

$$\sigma(q = 0, \omega = 0)/B(\alpha) = K(E_p, \omega = 0)\,|J_\alpha|^2 \exp(-xA^{1/2} + a_0). \quad (23)$$

Here, $K(E_p, \omega) = (E_i E_f/(\hbar^2 c^2 \pi)^2)(k_f/k_i)$ is a kinematic factor, and J_α is the exchange integral of the effective interaction $(\tau_1 \cdot \tau_2)$ or $(\sigma_1 \cdot \sigma_2)$ $(\tau_1 \cdot \tau_2)$. The dependence on the target mass (A) is given in the exponential, in which $x = 4W_i r_0(\hbar c \beta_i)$, W is the depth of the imaginary part of an optical potential of range r_0, and $\beta = \hbar c k/E$.

For the second factor we have the expression

$$F(q, \omega) = \frac{k(E_p, \omega)}{k(E_p, 0)} \exp\left(-\frac{1}{3} q^2 \langle r^2 \rangle\right) \exp[p(\omega) - a_0], \quad (24)$$

where $p(\omega) = a_0 + a_1\omega + a_2\omega^2$. It can be seen that in the limit $q, \omega \to 0$ the factor $F(q, \omega)$ tends to unity.

The β-transition strength is $B(\alpha)$. If the lifetime is known, it can be calculated in accordance with the expression

$$(G_V)^2 B(F) + (G_A)^2 B(GT) = \frac{K}{ft}, \quad (25)$$

where $K/G_V = 6166$ sec and $(G_A/G_V)^2 = 1.260^2$.

Numerous investigations of the (p, n) reaction made at intermediate energies with the cyclotron of the University of Indiana in the United States[2,3,16–26] have shown that Gamow–Teller transitions are dominant in the spectra measured at angle 0°, while isobar analog states are weakly excited. As was expected, the ratio $\sigma(0°)/B(GT)$ was found to be constant for a given spectrum, and, therefore, the differential cross sections at angle 0° can serve as a measure of the strength of the Gamow–Teller transitions. This is illustrated by the example of the ^{27}Al$(p, n)^{27}$Si reaction, which is shown in Fig. 4, taken from Ref. 16.

However, if we compare $\sigma(0°)/B(GT)$ and $\sigma(0°)/B(F)$ for different nuclei, then, as was shown in Ref. 16, a considerable spread of these values is found (Fig. 5), and this spread cannot be reproduced by distorted-wave calculations, which give a smooth dependence on A. The reason for this is still obscure. Thus, extrapolation or interpolation from nucleus to nucleus of the constants $\hat{\sigma}_{GT}$ and $\hat{\sigma}_F$, which relate the cross sections to the transition strengths in Eq. (22), can be done presently only with an error of ~20–50%.

The relatively weak excitation of isobar analog states in the (p, n) reaction at intermediate energies can be readily understood by plotting

$$R(E_p) = (\hat{\sigma}_{GT}/\hat{\sigma}_F)^{1/2}$$

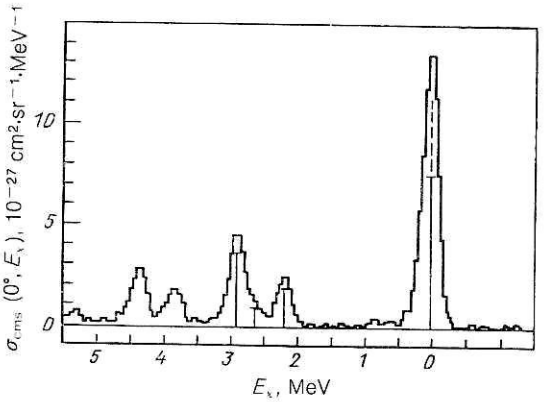

FIG. 4. Energy spectrum of the ^{27}Al$(p, n)^{27}$Si reaction obtained with 120-MeV protons at angle 0°. The height of the vertical lines is proportional to the strength of the Gamow–Teller transitions. The broken line shows the expected contribution of the Fermi transitions.

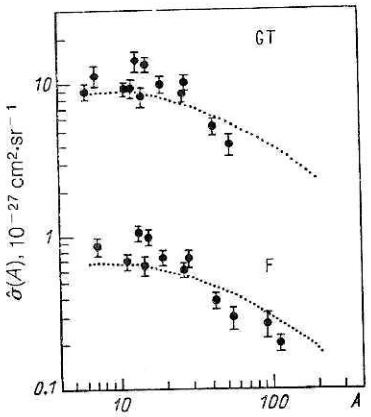

FIG. 5. Cross sections of the (p, n) reaction, normalized to unit transition strengths $B(GT)$ and $B(F)$, at proton energy 200 MeV. The curves are drawn through the points.

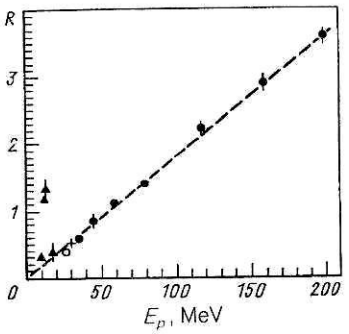

FIG. 6. Ratio of the strengths of the spin–isospin (GT) and isospin (F) interactions as a function of the proton energy.

as a function of the proton energy. The best source of information about such states is the $^{14}C(p, n)^{14}N$ reaction, for which measurements have been made of the cross sections of the transitions to the states 0^+ (2.3 MeV, isobar analog state) and 1^+ (3.95 MeV, Gamow–Teller resonance) in the interval $E = 12$–200 MeV. The values of $R(E_p)$, obtained for this case and calculated from the expression

$$R^2(E_p) = \frac{\sigma_{GT}(0^0)/B(GT)}{\sigma_F(0^0)/B(F)}, \qquad (26)$$

are shown in Fig. 6, which is taken from Ref. 16. We observe a linear dependence on E_p, $R(E_p) = E_p/(55.4 \pm 0.4)$, where E_p is expressed in mega-electron-volts.

The same dependence is observed for other targets. If we return to the expression in which $R(E\ )$ is expressed in terms of the ratio $\hat{\sigma}_{GT}/\hat{\sigma}_F$, then we readily see that this energy dependence can be related to the ratio $|J_{\sigma\tau}/J_\tau|$. Therefore, the dynamics of the (p, n) reaction is such that as the proton energy is increased the importance of the spin–isospin interaction increases, so that at energies above 100 MeV the Gamow–Teller transitions $(S = 1, T = 1)$ dominate over the isobar analog states $(S = 0, T = 1)$.

The selectivity of the (p, n) reaction at intermediate energies to Gamow–Teller transitions that we noted above, and also the fact that the cross sections at angle 0° were found to be proportional to the strength of these transitions, made it possible to investigate the spin–isospin structure of a large number of nuclei. Figure 7 shows typical neutron spectra obtained by the time-of-flight method at angle 0° at proton energy 200 MeV for a number of intermediate and heavy nuclei.[26,27] The isolated peaks observed in the spectra are associated with the excitation of collective 1^+ states, namely, Gamow–Teller resonances. Thus, the Gamow–Teller strength is concentrated in a relatively narrow range of excitation energies of the nuclei.

For the spin–isospin excitation mode there exists a very simple sum rule, which follows from the commutation relation for the operators t_+ and t_-:

$$S_{\beta^-} - S_{\beta^+} = 3(N - Z), \qquad (27)$$

where S_β is the strength of the β^- (and β^+) transitions, summed over all states. For nuclei with large neutron excess, S_{β^+} is small, since all the final states associated with transformation of a proton into a neutron are blocked.

Figure 8 shows the fractions of exhaustion of the sum rule observed in the (p, n) reaction at $E_p = 160$ MeV in the region of excitation energies $E_x < 30$ MeV.[27] It can be seen that experimentally only about 50% of the theoretically predicted strength was found. Two possible reasons for the weakening of the Gamow–Teller transitions are currently being discussed. The first arises from the existence of inter-

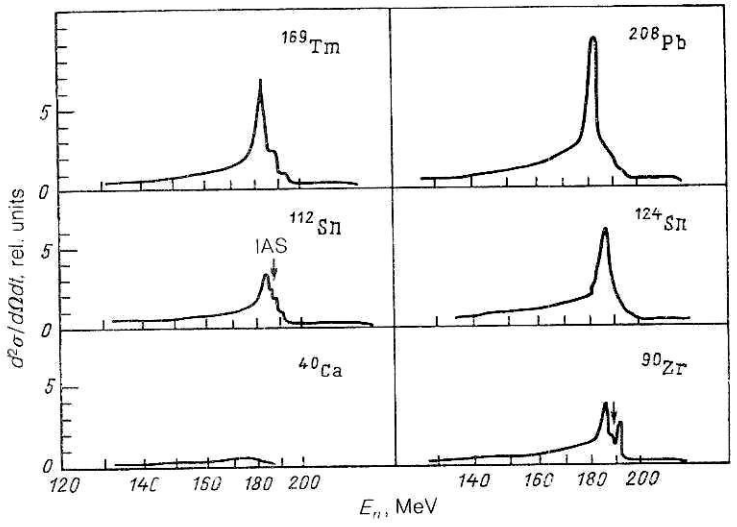

FIG. 7. Energy spectra of neutrons from the (p, n) reaction, obtained at proton energy 200 MeV at angle 0° on different nuclei.

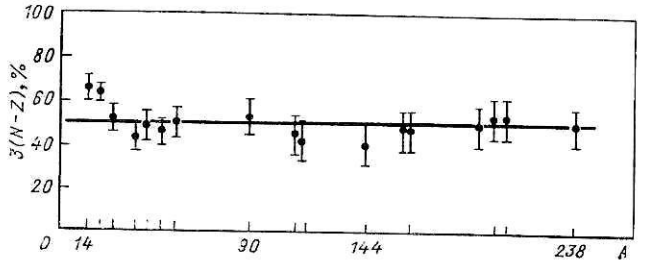

FIG. 8. Fractions of exhaustion of the sum rule for the Gamow–Teller transitions in the (p, n) reaction at $E_p = 160$ MeV.

nal structure of the nucleon, as a result of which the neutron can be transformed by the same spin–isospin interaction into the Δ isobar. The second possibility is associated with mixing of simple particle–hole excitations with more complicated configurations. Both possibilities can have the result that some of the Gamow–Teller strength is shifted to higher excitation energies or is smeared over the spectrum and thus becomes indistinguishable from the background. Recently discovered[28] variations of the coefficient of the weakening as a function of the filling of shells clearly indicate the importance of configuration mixing, at least for a number of cases.

The (^{3}He, t) reaction

The next reaction in which, as in the case of (p, n), a neutron of the target nucleus can undergo charge exchange into a proton is (^{3}He, t). Investigations made with the cyclotrons at Jülich,[29-31] Grenoble,[32] Groningen,[33] and Maryland[34] have shown that this reaction excites the same states as the (p, n) reaction, but at energies of the ^{3}He ions at least below 200 MeV the charge-exchange mechanism in the inclusive spectrum of the tritons is only a small fraction of the cross section. The sought-for structure of the particle–hole excitations is situated over a very strong background, which, according to Refs. 30, 31, and 33, is probably associated with breakup of the ^{3}He nucleus (^{3}He, dp) and subsequent (d, t) pickup. For this reason, the analysis of the spectra of the (^{3}He, t) reaction at $E_{^3\mathrm{He}} < 200$ MeV is often ambiguous, and here the (^{3}He, t) reaction is ineffective as a method for the study of isobaric transitions.

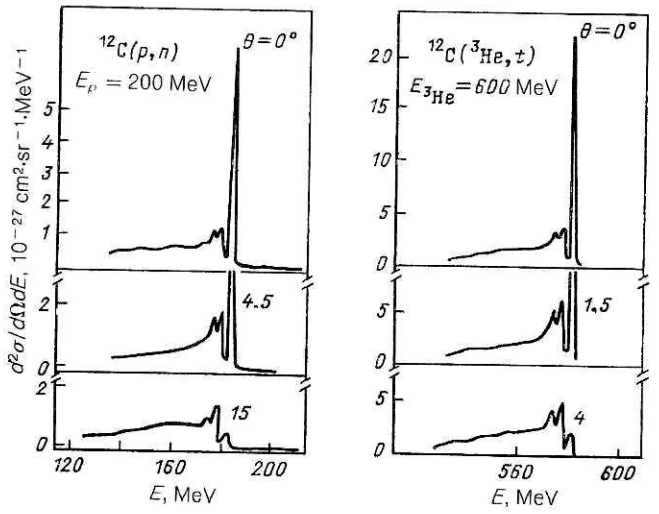

FIG. 9. Comparison of spectra of the (p, n) and (^{3}He, t) reactions on the ^{12}C nucleus, obtained at energy 200 MeV/nucleon of the incident particle.

As the beam energy is increased, the one-step charge-exchange mechanism can be better separated. In Fig. 9 we compare the spectra of the (p, n) and (^{3}He, t) reactions, obtained at energy 200 MeV per nucleon on the ^{12}C nucleus.[35] The angles are chosen in such a way that the momentum transfers in the two reactions are the same. Under these conditions the (^{3}He, t) and (p, n) reactions are obviously equivalent.

For all that, the (^{3}He, t) reaction does have a region of application in which as yet no other reaction can compete with it. Using ^{3}He beams of several giga-electron-volts from the accelerator Saturn at Saclay[36,37] and the synchrophasotron at the Joint Institute for Nuclear Research, Dubna,[38,39] it proved possible to investigate nuclei at excitation energies around 300 MeV, corresponding to a $(\sigma\tau)$ transition of a nucleon into a Δ isobar. However, discussion of this question goes beyond the scope of the present review.

The (n, p) reaction

Charge-exchange excitations in which the neutron excess is increased can in principle be studied using beams of light particles on the basis of the (n, p), $(d, {}^2\mathrm{He})$, and $(t, {}^3\mathrm{He})$ reactions. However, the spectra published for the last reaction are restricted to a comparatively narrow interval of excitation energies[40] on account of technical difficulties in obtaining high-energy beams of radioactive tritium.

The first reaction was investigated with the cyclotron of the University of California at neutron energies of about 60 MeV. A quasimonoenergetic neutron beam was obtained by means of the ^{7}Li$(p, n)^7$Be reaction. Usually, its intensity was 10^6 sec^{-1} with an energy resolution around 1 MeV. Measurements were made on many target nuclei, from ^{4}He to ^{209}Bi (Refs. 41–45). The main result of the investigations was the discovery in the experimental proton spectra of structures corresponding to giant dipole resonances of the target nuclei. The fact that reactions of the (n, p) type select $T_0 + 1$ states, where T_0 is the isospin of the target nucleus, makes them a promising tool for the study of the isotopic splitting of giant resonances.

With regard to the (n, p) reaction itself, it should be said that its possibilities are severely restricted. First, the intensity of the neutron beams is too low. As a rule, the intensity is 10^6 times lower than that of the beams of charged particles generally employed. In addition, the energy profile of the beams is not, strictly speaking a monoline, but also contains a continuous component, which makes a significant contribution to the total cross section. Second, the resonance structure at $E_n < 100$ MeV is situated on a very intense distribution associated with multistep processes, and this distribution increases strongly with the excitation energy. An example of a typical spectrum of the ^{90}Zr$(n, p)^{90}$Y reaction is shown in Fig. 10a. Third, and last, the (n, p) reaction at $E_n < 100$ MeV does not possess selectivity with respect to spin flip. Transitions with both $S = 0$ and $S = 1$ occur equally in it. Taken altogether, these factors introduce a significant uncertainty into the estimate of the background and into the analysis and interpretation of the results.

These limitations can be partly overcome in experiments with the neutron beams obtained recently with the TRIUMF facility,[46-49] which make it possible to investigate the (n, p) reaction at intermediate energies (200–500 MeV). Neutron beams with energy up to 800 MeV have also recent-

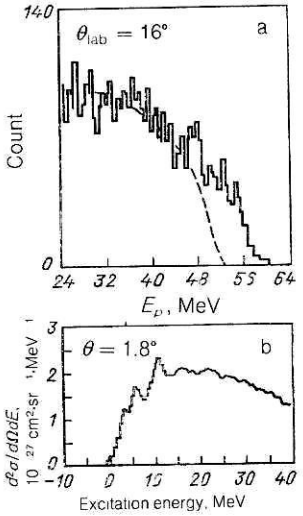

FIG. 10. Energy spectra of protons from the ^{90}Zr$(n,p)^{90}$Y reaction: a) E_n = 59.4 MeV; b) E_n = 198 MeV at angle 1.8°.

ly become available at the meson factory at Los Alamos, and with energy up to 200 MeV at the cyclotron at Uppsala in Sweden[51] and at the cyclotron of the University of Indiana.[52] At such energies, the (n,p) reaction becomes selective with respect to transitions with spin flip ($S=1$). In addition, with increasing beam energy the maximum of the background from the multistep processes must be shifted to higher excitation energies, and this changes the signal-to-background ratio in favor of the one-step charge-exchange mechanism in, at least, the hard part of the spectrum.

Figure 10b shows the energy spectrum of the ^{90}Zr$(n,p)^{90}$Y reaction obtained at angle 1.8° at neutron energy 198 MeV.[47] The maxima observed at $E_x \simeq 5$ and 10 MeV are associated with the dominant excitation of a spin-dipole resonance ($L=1$, $S=1$). Note that these maxima are not observed in the analogous spectra measured at E_n = 59.4 MeV (Fig. 10a). Instead we observe a group with center at $E_n \sim 7$ MeV corresponding to excitation of the $T_>$ component of the ordinary dipole (without spin flip) resonance. The neutron excess leads to an appreciable asymmetry in the charge-exchange transitions in which the charge is increased ($\Delta T_z = -1$) or decreased ($\Delta T_z = +1$). Whereas in (p,n) a Gamow–Teller resonance is dominant in the energy spectra measured at angle 0° (see Fig. 7), in the inverse (n,p) reaction on heavy nuclei strong Gamow–Teller transitions should not be observed, since the neutron subshell $\nu j_{l-1/2}$, to which these transitions could take place from the proton subshell $\pi j_{l+1/2}$ is already occupied. This facilitates investigation of spin-dipole and other resonances of higher multipolarity.

The $(d, {}^2\mathrm{He})$ reaction

Whereas in the (n,p) reaction selectivity to spin-flip transitions arises only at higher beam energies, in the case of the $(d, {}^2\mathrm{He})$ reaction it exists from the very beginning and is due to the structure of the deuteron, which has the quantum numbers $(LST) = (010)$ and a system of two unbound protons. It is merely necessary to make an experiment with protons in coincidence with a small relative energy, when the main contribution is made by the singlet state ($LST = 001$). The $(d, {}^2\mathrm{He})$ reaction has been studied at $E_d = 55$ MeV (Ref. 53), $E_d = 99$ MeV (Ref. 54), 70 MeV (Ref. 55), and 650 MeV (Ref. 35) using several light nuclei from ^{6}Li to ^{14}N, and the selectivity of this reaction to spin-flip transitions has been fairly well demonstrated. However, this reaction too has its methodological difficulties, which explain why there are still no systematic investigations on intermediate and heavy nuclei. The main problem in the measurements is that the most probable process with deuterons is disintegration, which gives a large number of single protons accompanying correlated pairs. Therefore, in a $(d, {}^2\mathrm{He})$ experiment it is necessary to select these pairs by coincidence, and this leads to a loss of efficiency and difficulties in determining the absolute value of the cross section.

Thus, none of the charge-exchange reactions with light ions considered in this section can completely satisfy us, particularly as regards the reactions in which the neutron excess is increased.

4. INVESTIGATIONS OF THE (^{6}Li, ^{6}He) REACTION

The (^{6}Li, ^{6}He) reaction at low energies

The first investigation of the (^{6}Li, ^{6}He) reaction was made in 1970 at the cyclotron of the I. V. Kurchatov Institute of Atomic Energy. The energy of the beam of ^{6}Li ions was 32 MeV.[4,5]

The energy spectra measured on the nuclei ^{7}Li, ^{7}Be, and ^{13}C (Fig. 11) were in fairly good qualitative agreement with the assumption of a quasielastic reaction in which the odd neutron is transformed into a proton solely through forces that change the spin and isospin.

Later, at beam energies 30–40 MeV, the (^{6}Li, ^{6}He) reaction was studied more systematically.[56–65] It was established that the one-step charge-exchange mechanism explains the greater part of the observed cross sections. However, there were some reports of appreciable variation of the strength parameter of the spin–isospin interaction $V_{\sigma\tau}$ deduced from the analysis; it was found to take unrealistically large values, particularly for normal-parity states. There were also reports of the excitation of 0^+ states, forbidden in

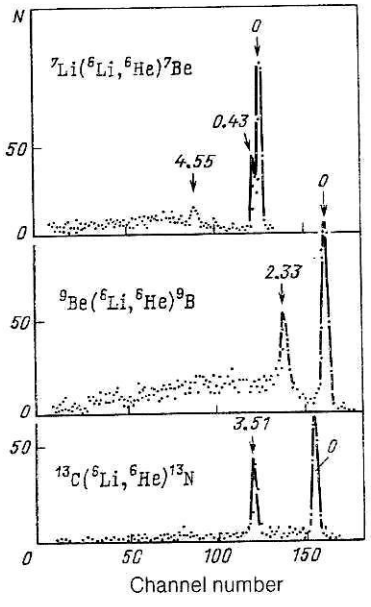

FIG. 11. Energy spectra of the (^{6}Li, ^{6}He) reaction on the nuclei ^{7}Li, ^{9}Be, and ^{13}C, obtained at energy 31.8 MeV of the ^{6}Li ions at angle $\theta_{lab} = 12°$.

the one-step mechanism, whose differential cross sections could reach 10% of the corresponding values of the strongest transitions. These facts indicate that at energies 30–40 MeV the (^{6}Li, ^{6}He) mechanism is more complicated. For example, 10% of the cross section of the ^{14}C(^{6}Li, ^{6}He) reaction was explained in the analysis of Ref. 64 by a mechanism with formation of a compound nucleus. Other work[58-60] indicated that quasidirect multistep processes make an important contribution to the reaction. These processes can be divided into two types. The first is associated with charge exchange, which precedes Coulomb excitation or follows it. The second is associated with successive transfer of one nucleon from the target nucleus to the incident particle and back (^{6}Li–^{7}Li–^{6}He). It is obvious that the second process must have a larger cross section, since in both the first and the second stage strong single-nucleon transfer is involved.

Mechanism of the (^{6}Li, ^{6}He) reaction at $E/A > 10$ MeV

The mechanism of the (^{6}Li, ^{6}He) reaction at higher energies was investigated in detail in Ref. 12. Measurements were made on a ^{14}C target, and the energy of the lithium ions was 93 MeV. The angular distributions obtained for a number of anomalous-parity states of the ^{14}N nucleus (1^+, 2^-, 4^-) were analyzed in the framework of the one-step charge-exchange mechanism as described in Sec. 2. The form factor was calculated using only a central potential reponsible for spin flip, $f(r)(\sigma_p\sigma_t)\cdot(\tau_p\tau_t)$, and shell-model wave functions. Figure 12, which is taken from Ref. 12, compares the experimental and theoretical angular distributions for transitions to the ground state and excited 1^+ state of the ^{14}N nucleus at beam energies 62 and 93 MeV.

Experimental data for 62 MeV were obtained in Ref. 11. Equally good descriptions of the shape of the angular distributions were obtained for two forms of the interaction $f(r)$. In the case of a potential of Gaussian form $f(r) = V_{\sigma\tau}e^{-r^2/a^2}$ ($a = 1.8$ F), the theoretical absolute cross sections agreed with the experimental cross sections for interaction strength $V_{\sigma\tau} = 10.7$ MeV. A similar result was obtained in Ref. 64, but for measurements with the energy of the lithium ions in the range 30–60 MeV. Thus, the interaction strength deduced from the experiments does not vary in the range of beam energies 30–90 MeV, and it is also independent of the excitation energy.

The strength of the spin–isospin interaction given above is in reasonable agreement with a further empirical estimate, $V_{\sigma\tau} \simeq 300g'/(\pi^{3/2}a^3)$ (Ref. 66), if in this expression we substitute the value of the Landau–Migdal constant found from the position of the Gamow–Teller resonance in a number of nuclei, namely, $g' = 1.1$ (Ref. 67).

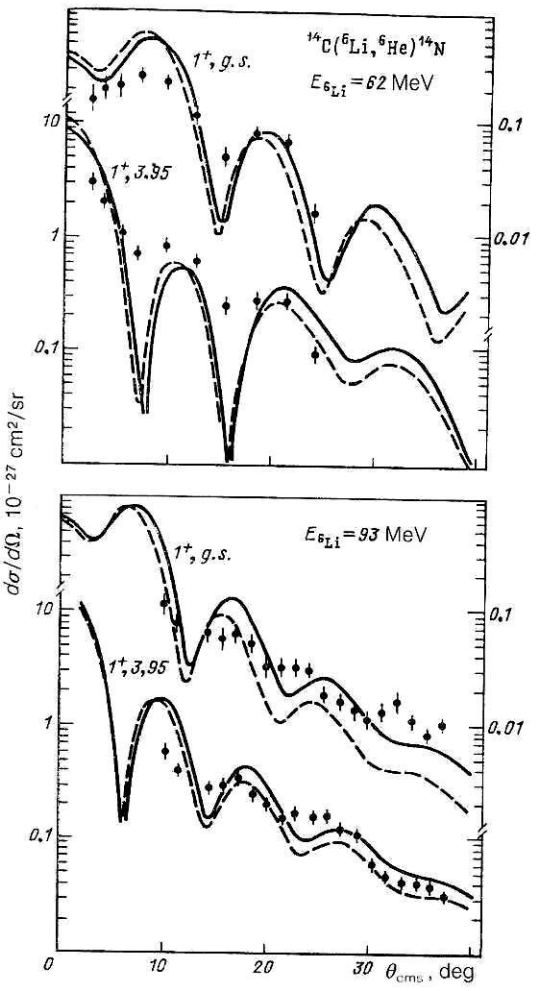

FIG. 12. Angular distributions of ^{6}He nuclei from the ^{14}C(^{6}Li, ^{6}He)^{14}N reaction for transitions to 1^+ states with E_x equal to 0 and 3.95 MeV and energies 62 and 93 MeV of the lithium ions. The continuous curve is a calculation with a Gaussian interaction ($V_{\sigma\tau} = 10.7$ MeV), and the broken curve is calculated with the M3Y interaction (in the second case the calculated cross sections have been multiplied by 1.7).

In another version, the interaction was represented as a superposition of Yukawa potentials with an additional term to imitate exchange effects and with the parameters of Ref. 6 (interaction M3Y). To achieve agreement between theory and experiment, the theoretical cross sections had to be multiplied by $N = 1.7$; in the first place, this could have been due to neglect of tensor forces in the calculations. It should be noted that additional normalization factors must also be introduced for an interaction of Gaussian form in the case of transitions to states with the large spin values 2^- ($N = 2$)

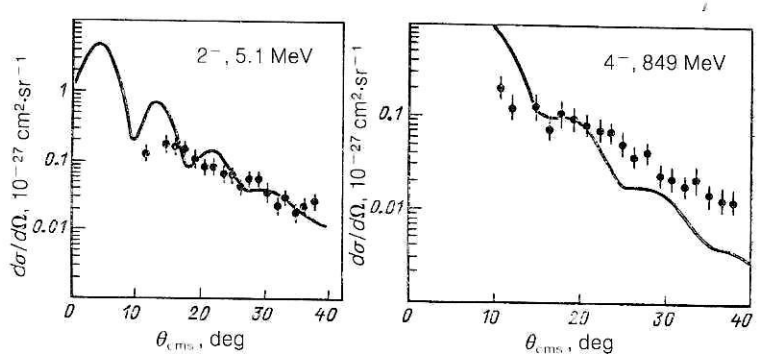

FIG. 13. Angular distributions of ^{6}He nuclei from the ^{14}C(^{6}Li, ^{6}He) reaction for transitions to the states 2^- ($E_x = 5.1$ MeV) and 4^- ($E_x = 8.49$ MeV). The continuous curves are calculated with a Gaussian interaction. The theoretical cross sections have been multiplied by a coefficient 2 in the first case and 3 in the second.

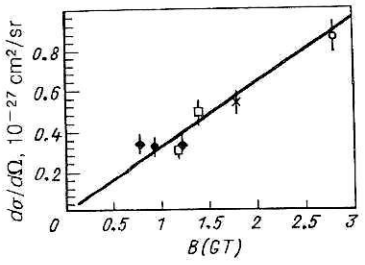

FIG. 14. Differential cross sections of Gamow–Teller transitions at a fixed value of qR ($q = 100$ MeV/c for a ^{14}C target) as functions of $B(GT)$. The final nuclei are indicated in the figure as follows. Open circles for ^{14}N ($E_x = 3.95$ MeV), crosses for ^{90}Nb (2.3 MeV), black circles for ^{12}N (0.0 MeV), open squares for ^{7}Be (0 and 0.43 MeV), and black diamonds for ^{26}Al (1.06 and 1.85 MeV).

and 4^- ($N = 3$) in the ^{14}C(^{6}Li,^{6}He)^{14}N reaction (Fig. 13).

Recently, the (^{6}Li, ^{6}He) reaction was investigated on a number of nuclei at beam energy 210 MeV.[68] The transition to the 1^+ state ($E_x = 3.95$ MeV) of the ^{14}N nucleus was analyzed by means of the Yukawa interaction $f(r) = V_{\sigma\tau} e^{-r/a}/(r/a)$ with length parameter $a = 1.0$ F. Both central and tensor forces were taken into account. Normalization to the experiment gave $V_{\sigma\tau} = 14.4$ MeV, which is fairly close to the value 11.7 ± 1.7 MeV obtained from the (p, n) reaction at the same value of the energy per nucleon.[69]

If the (^{6}Li, ^{6}He) reaction is realized by the direct one-step mechanism, then the differential cross sections measured for Gamow–Teller transitions at some fixed momentum must be proportional to the Gamow–Teller strength. As is shown in Fig. 14, which is taken from Ref. 68, there is indeed a clearly expressed correlation between the differential cross sections at the second diffraction peak of the angular distributions ($q = 100$ MeV/c for ^{14}C) and the known values of $G(GT)$. Thus, the graph of Fig. 14 is actually an empirical calibration by means of which one can determine the strength of Gamow–Teller transitions from measured differential cross sections. The question arises of the extent to which the empirical dependence found at $E = 210$ MeV is suitable for other energies of the bombarding particles. The answer depends on the magnitude of the differences in the distortions of the wave functions of the relative motion. Figure 15 compares the angular distributions for the transition to the 1^+ state with excitation energy 3.95 MeV of the ^{14}N nucleus measured for three energies of the ^{6}Li ions: 62 MeV (Ref. 11), 93 MeV (Ref. 12), and 210 MeV (Ref. 68). The angular distributions are constructed in the scale of the momentum transfer without additional normalization. It can be seen from Fig. 15 that in all three cases the same diffraction structure, with peaks for $q = 0.5$ and 1 F^{-1} is observed. However, whereas the angular distributions for the energies 62 and 93 MeV are the same in the complete measured range of momentum transfers, at 210 MeV the differential cross sections in the region of the first and third diffraction peaks are significantly smaller than in the first two cases. The discrepancy between the relative values of the differential cross sections at 62 and 93 MeV, on the one hand, and 210 MeV, on the other, is reproduced by theoretical calculations with distorted waves and, therefore, can be completely explained by effects of distortions. We note at the same time that the distortions do not vary strongly as the energy of the ^{6}Li ions is varied from 60 to 210 MeV; such variation leads to a decrease of the cross sections by a factor of about 2 only in the regions of the first and third diffraction peaks. Thus, apart from a factor, the two differential cross sections of the (^{6}Li, ^{6}He) reaction characterize the strength of the Gamow–Teller transitions at any energy of the ^{6}Li ions from 60 to 210 MeV.

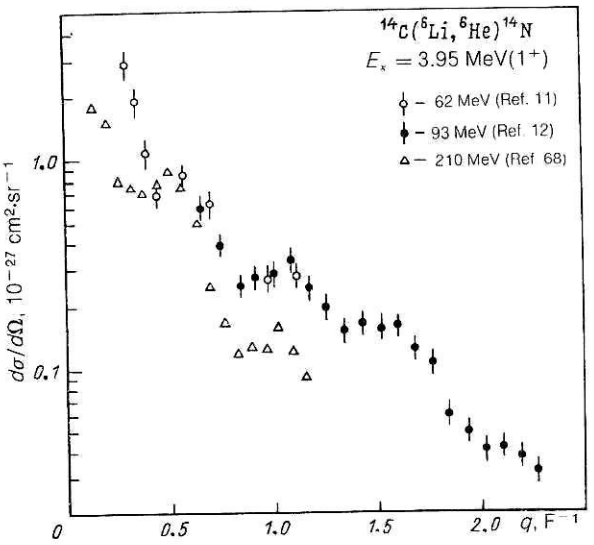

FIG. 15. Angular distributions for transition to the 1^+ state with excitation energy 3.95 MeV of the ^{14}N nucleus, plotted in the scale of the momentum transfer.

A good additional test of the (^{6}Li, ^{6}He) reaction mechanism is comparison of the cross sections for excitation of the 0^+ state at 2.31 MeV, which is forbidden in the one-step charge-exchange mechanism, and the 1^+ state at 3.95 MeV of the ^{14}N nucleus. As the beam energy is changed, their ratio, measured at small angles, is 0.05 at $E/A = 35$ MeV/nucleon and 0.1 at $E/A = 10$ MeV/nucleon according to Ref. 68. A comparison that we made in a larger range of angles (10–30°) shows that this ratio changes appreciably already for an increase of the energy E/A from 10 to 15 MeV/nucleon, decreasing by a factor of about 2. This fact indicates that the multistep processes become less important with increasing beam energy.

Thus, all the currently available data indicate that at least at energies above 10 MeV/nucleon the direct one-step charge-exchange mechanism with spin flip is dominant in the (^{6}Li, ^{6}He) reaction.

The (^{6}Li, ^{6}He) reaction on intermediate nuclei

The direct one-step mechanism of the (^{6}Li, ^{6}He) reaction makes it possible to use this reaction as a probe of the spin–isospin structure of heavier nuclei. Figure 16 shows examples of spectra of the (^{6}Li, ^{6}He) reaction obtained on ^{52}Cr, ^{90,91}Zr, ^{120}Sn targets at beam energy 93 MeV. The spectra are similar, and in all cases we observe broad distributions with maxima orresponding to excitation energies 10–15 MeV of the residual nuclei. Comparison of the energy spectra of the (^{6}Li, ^{6}He) and (p,n) reactions studied at proton energies above 100 MeV under conditions for which the spin–isospin component of the interaction is dominant (Fig. 17) demonstrates their important differences. Whereas in the (p, n) reaction at $\theta = 0°$ the Gamow–Teller resonance is predominantly excited, in the ^{90}Zr(^{6}Li, ^{6}He) reaction a more complicated structure is observed, though the maxi-

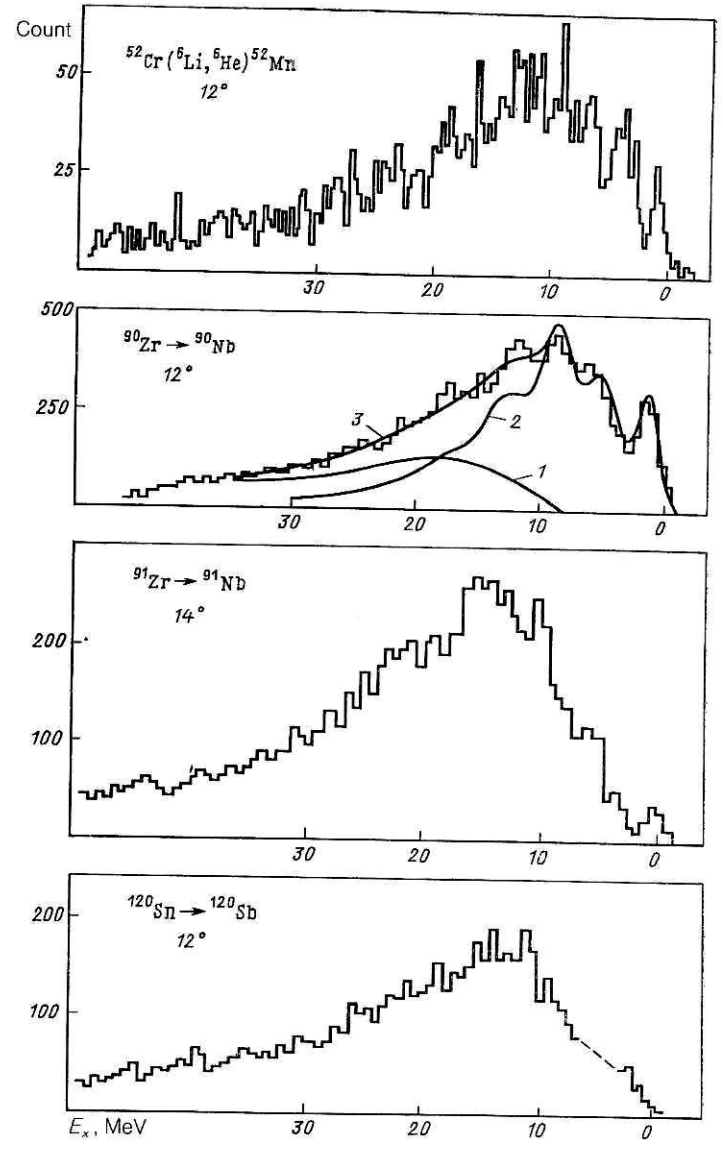

FIG. 16. Energy spectra of ^{6}He nuclei from the (^{6}Li, ^{6}He) reaction on ^{52}Cr, ^{90,91}Zr, and ^{120}Sn targets, obtained at beam energy 93 MeV: 1) the assumed contribution of the two-step process of the type $^{6}\text{Li} + {}^{90}\text{Zr} \rightarrow {}^{7}\text{Li}^{*} + {}^{89}\text{Zr} \rightarrow {}^{6}\text{He} + p + {}^{89}\text{Zr}$; 2) the contribution of the one-step charge-exchange process; 3) the sum of contributions 1 and 2.

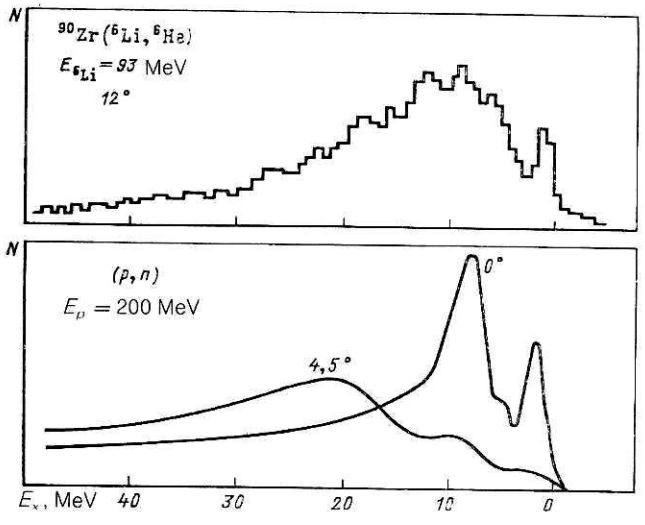

FIG. 17. Comparison of the energy spectra of the (^{6}Li, ^{6}He) and (p, n) reactions. The spectrum of the (p, n) reaction is taken from Ref. 2.

mum of the spectrum is at the Gamow–Teller resonance. The main reason for the difference between the (^{6}Li, ^{6}He) and (p, n) spectra is that they were investigated in different ranges of the momentum transfer (Fig. 18), so that in the (^{6}Li, ^{6}He) reaction transitions with a large value of the orbital angular momentum were kinematically preferred. For nearly equal momentum transfer the difference between the (^{6}Li, ^{6}He) and (p, n) spectra can be due to the difference between the physical backgrounds, which in the first case is expected to be smaller than in the second. Moreover, it must always be borne in mind that the (^{6}Li, ^{6}He) reaction has a more rigorous selectivity with respect to spin-flip transitions.

The ^{90}Zr(^{6}Li, ^{6}He)^{90}Nb reaction was investigated in detail in Ref. 66. Because the observed structure was complicated, the spectra were analyzed by dividing them into individual sections without subtracting any background. The angular distributions for each energy interval were calculated in the framework of the microscopic distorted-wave

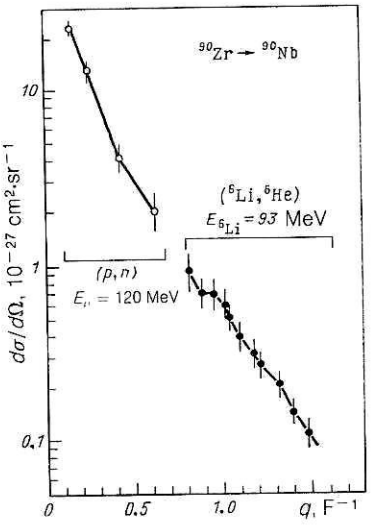

FIG. 18. Differential cross sections of the Gamow–Teller resonance, measured in the (p, n) reaction[2] and (^{6}Li, ^{6}He) reaction on ^{90}Zr. The abscissa is the scale of the momentum transfers.

method with a central spin–isospin interaction potential, in which the coordinate part was described by a Gaussian function; as a result the recoil effects in the light system could be taken into account fairly easily. The transition densities of the target nucleus, which occur in the form-factor integrals [see Eq. (13)], were calculated on the basis of the theory of finite Fermi systems.[67] All the levels and resonances of the particle–hole structure up to $J^\pi = 8^-$ were taken into account in the calculations of the cross sections. The theoretical angular distributions obtained for $V_{\sigma\tau} = 10.7$ MeV are given in Fig. 19. The contributions of all multipolarities from 0 to 6 and the total angular distributions are shown together with the experimental points. It can be seen that in all sections a restriction can be made to the contributions of the multipolarities $\leqslant 5$; the contributions of the higher multipolarities decrease rapidly. It can also be seen that there is no section in which one particular multipolarity makes a dominant contribution. Thus, in the section $E_x = 7$–11 MeV transitions with $\Delta L = 2$ and 3 are important, along with the Gamow–Teller resonance and the spin-dipole transitions.

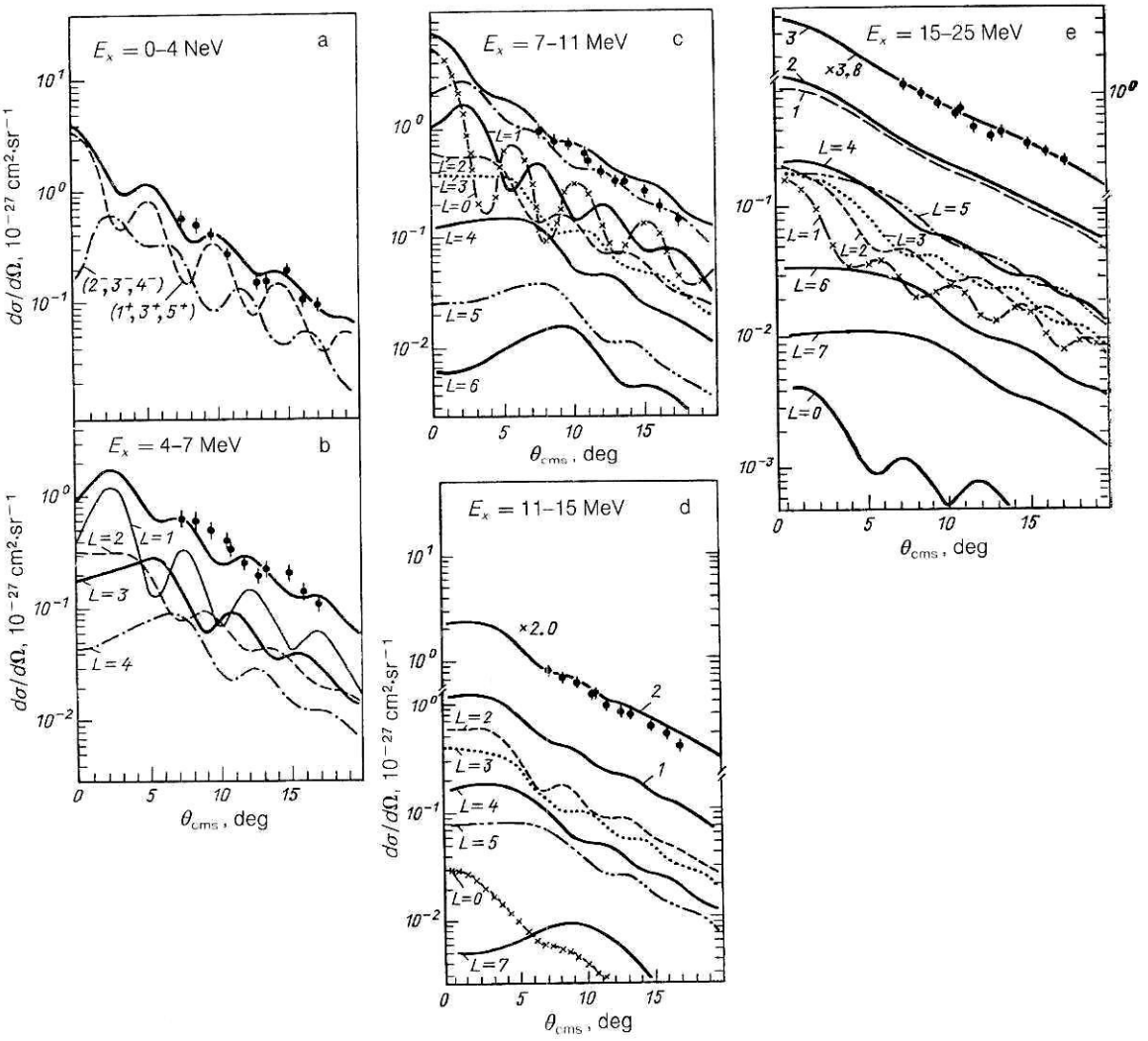

FIG. 19. Angular distributions of ^{6}He nuclei from the reaction ^{90}Zr(^{6}Li, ^{6}He)^{90}Nb. The curves give the theoretical calculation with a Gaussian interaction. The partial contributions from excitation with multipolarity L are shown. In (d) curve *1* is the total theoretical angular distribution, while curve *2* is the same distribution normalized to the experiment, $N = 2$. In (e) curve *1* is the total contribution of all the multipolarities except $L = 1$; curve *2* is the total theoretical cross section; curve *3* is the distribution normalized to the experiment, $N = 3.8$.

At higher excitation energies, the contribution of the transitions having ΔL equal to 0 and 1 decreases, giving not more than 10–15% of the total cross section, so that in the section $E_x = 15$–25 MeV the nature of the angular distribution is basically determined by the multipolarities $L = 4$ and $L = 5$.

Comparison of the total theoretical angular distributions with the experimental distributions shows that up to $E_x \sim 11$ MeV the calculations agree well with the experiment. The nature of the angular distributions is also correctly described at higher excitation energies, but the difference between the experimental absolute cross sections and the theoretical values obtained for $V_{\sigma\tau} = 10.7$ MeV increases rapidly. Thus, in the region $E_x = 11$–15 MeV the theoretical cross section is 50% of the experimental one, but in the region $E_x = 15$–25 MeV it is only 26%. This fact can be understood by assuming that in these regions processes different from the one-step charge-exchange mechanism begin to play a part.

The part played by the quasielastic processes is more clearly revealed by comparing the theoretical and experimental energy spectra (Fig. 16). The theoretical spectrum was obtained by introducing a smearing of Breit–Wigner type:

$$\frac{d^2\sigma}{dE\,d\Omega} = \sum_i \left(\frac{d\sigma}{d\Omega}\right)_i \frac{1}{2\pi} \frac{\Gamma_i}{(E-\overline{E}_{x_i})^2+\Gamma_i^2/4}, \qquad (28)$$

where $(d\sigma/d\Omega)_i$ is the total differential cross section at angle θ in the energy interval i. The expression (28) is the sum of the contributions of all the multipolarities in this interval; $\overline{E}_{x_i}$ are the centroid energies, taken to be $\overline{E}_x = 1.5$, 5.6, 8.8, 13.0, and 18.0 MeV in accordance with the nature of the spectra observed in the (^{6}Li, ^{6}He) reaction. It can be seen from Fig. 16 that the assumption of a quasielastic reaction mechanism (curve *2*) leads to a good description of the low-energy part of the spectra up to $E_x \simeq 10$ MeV. Thereafter the contribution of this mechanism decreases rapidly and is only a small fraction of the observed cross section. If from the experimental spectrum we subtract the theoretical spectrum corresponding to the direct one-step mechanism, then in what remains we obtain roughly a broad distribution with a maximum corresponding approximately to the excitation energy in the ^{90}Nb nucleus: $E_x \simeq 18$–20 MeV (curve *1*). This distribution can evidently be associated with other mechanisms ignored in the calculation. Among them the most probable is the two-step process involving pickup of one neutron into excited states of the ^{7}Li nucleus situated above the threshold of its disintegration into ^{6}He + p:

$$^{90}\mathrm{Zr} + {}^6\mathrm{Li} \rightarrow {}^{89}\mathrm{Zr} + {}^7\mathrm{Li}^* \rightarrow {}^{89}\mathrm{Zr} + {}^6\mathrm{He} + p.$$

The fact that the maximum of the observed distribution corresponds to the velocities of the excited ^{7}Li nuclei is evidence in support of this mechanism; moreover, the width of the maximum does not contradict the kinematic bounds for this two-step process.

The investigation of the ^{90}Zr(^{6}Li, ^{6}He) reaction in Ref. 66 also showed that the spin-flip transitions with $L \geqslant 2$ are strongly fragmented and do not form localized giant resonances, as they do for $L = 0$ and $L = 1$. But if we set ourselves the task of separating in the reactions with light ions resonance structures with definite multipolarities, then it is evidently promising to make measurements at small angles and

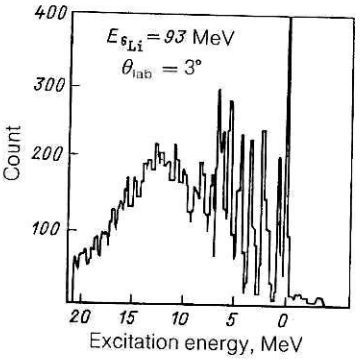

FIG. 20. Energy spectrum of the ^{27}Al(^{6}Li, ^{6}He)^{27}Si reaction at $E_{^6Li} = 93$ MeV.[70]

raise the beam energy appreciably in order to widen the region of excitation energy of the residual nucleus accessible to investigation. This requirement is dictated by the sharp decrease of the cross section of the quasielastic process with increasing excitation energy (Q dependence). Thus, for $E_{^6Li} = 93$ MeV the calculated cross section of the ^{90}Zr(^{6}Li, ^{6}He)^{90}Nb reaction for the quadrupole resonance in the region $E_x = 25$ MeV was about two orders of magnitude less than in the region $E_x = 18$ MeV.

An investigation of the (^{6}Li, ^{6}He) reaction on a ^{27}Al target was reported in Ref. 70. The energy of the ^{6}Li ions was also 93 MeV. An example of the spectrum of this reaction, measured at angle 3°, is shown in Fig. 20. In its form it is very similar to the spectra given in Fig. 16. Besides low-lying discrete groups of states, we observe a distribution with FWHM of about 10 MeV and centroid at $E_x \simeq 10$–12 MeV. The angular distribution for this structure is shown in Fig. 21. An analysis based on the microscopic distorted-wave method with an *NN* interaction of the type M3Y shows that the observed angular distribution can be explained by a mixture of multipolarities in the interval $L = 3$–5.

5. INVESTIGATION OF THE (^{7}Li, ^{7}Be) REACTION

The (^{7}Li, ^{7}Be) reaction on light nuclei

The simplest way to obtain a qualitative picture of the mechanism of the (^{7}Li, ^{7}Be) reaction is to compare its energy spectra with the spectra of the reference (^{6}Li, ^{6}He) reac-

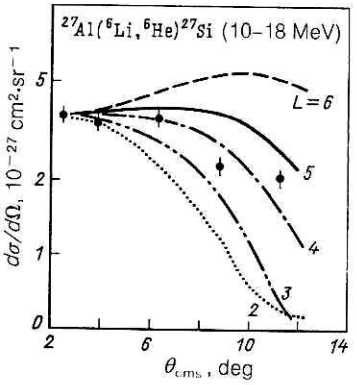

FIG. 21. Comparison of the experimental angular distribution for the broad group observed in the ^{27}Al(^{6}Li, ^{6}He)^{27}Si reaction at $E_x \sim 10$–12 MeV with theoretical calculations for different values of the orbital angular-momentum transfer L.

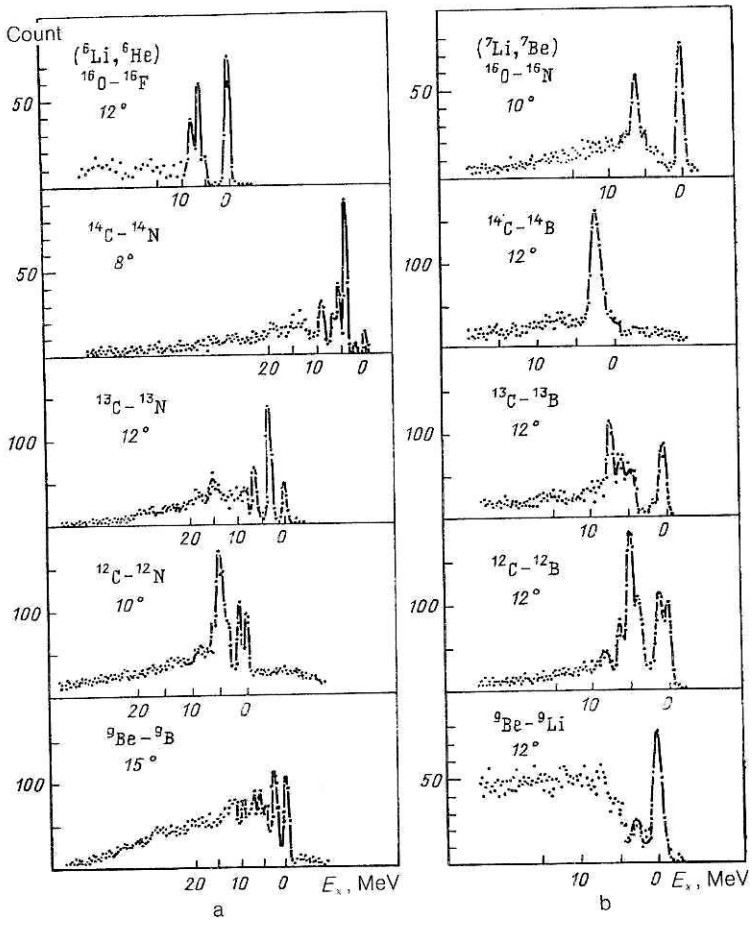

FIG. 22. Energy spectra of ^{6}He nuclei from (^{6}Li, ^{6}He) reactions on the nuclei ^{9}Be, ^{12,13,14}C, and ^{16}O (a). The energy spectra of the ^{7}Be nuclei from the (^{7}Li, ^{7}Be) reactions on the same nuclei (b).

tion, the mechanism of which can be regarded as established. Recently, these two reactions were investigated on the same nuclei, ^{9}Be, ^{12,13,14}C, and ^{16}O, under similar kinematic conditions.[71] Examples of spectra obtained for ^{6}Li energies of 93 MeV and ^{7}Li energies of 78 MeV are shown in Fig. 22. It is particularly interesting to compare the energy spectra of the (^{7}Li, ^{7}Be) and (^{6}Li, ^{6}He) reactions on the nuclei with $N = Z$: ^{12}C and ^{16}O. In this case, the conditions of charge exchange for a neutron and for a proton are the same, and, therefore, if the two reactions have the same mechanism, one can expect their spectra to be similar. It can be seen from Fig. 22 that in the spectra of the (^{6}Li, ^{6}He) and (^{7}Li, ^{7}Be) reactions on the ^{12}C and ^{15}O nuclei we do indeed observe the same level system of the mirror nuclei ^{12}N–^{12}B and ^{16}N–^{16}F. Moreover, the ratios of the differential cross sections between the individual groups of levels in the (^{7}Li, ^{7}Be) and (^{6}Li, ^{6}He) reactions are approximately the same. For (^{7}Li, ^{7}Be), as for (^{6}Li, ^{6}He), we note the predominant excitation of the anomalous-parity states 1^+, 2^-, and 4^-. This is a remarkable fact, since the selection rules given above by no means predict that spin-flip transitions should be kinematically distinguished in the (^{7}Li, ^{7}Be) reaction.

But if we compare the spectra of the (^{7}Li, ^{7}Be) and (^{6}Li, ^{6}He) reactions with the (p, n) and (n, p) spectra at approximately the same momentum transfers (Fig. 23), we can see that the spectra of both of the reactions with lithium are similar to the spectra of the (p, n) reaction obtained at a proton energy above 100 MeV, while they differ strongly for the (n, p) case at $E_n = 60$ MeV. The main difference is that in the (n, p) case transitions to 1^- and 2^- states occur most strongly. As we have already noted, the abrupt change in the nature of the excitation in (n, p) and (p, n) when the beam energies changed from 60 to 100 MeV is due to the dynamical features of charge-exchange reactions with nucleons, these being expressed by the fact that the ratio $V_{\sigma\tau}/V_\tau$ increases with increasing energy. This has the consequence that at energies above 100 MeV the spin–isospin charge-exchange mechanism is dominant.

The angular distributions for the strongest groups of states observed in the energy spectra of the ^{12}C(^{7}Li, ^{7}Be)^{12}B and ^{16}O(^{7}Li, ^{7}Be)^{16}N reactions for E_x equal to 4.5 and 6.2 MeV, respectively (Fig. 24), were analyzed in Ref. 13 in the framework of the microscopic distorted-wave method for one-step charge exchange (see Sec. 2). The calculation was made with central forces, the radial dependence of which was described by a superposition of Yukawa potentials with the addition of a term to imitate exchange effects. The transition density for the ^{7}Li–^{7}Be system was calculated in accordance with the ^{7}Li$(\alpha + t)$ and ^{7}Be$(\alpha + {}^3$He) cluster model with three "active" nucleons. The transition densities in the heavy systems ^{12}C–^{12}B and ^{16}O–^{16}N were calculated for several (experimentally forbidden) states (4^-, 3^-, 2^-, 1^-) with a simple particle–hole structure. Oscillator wave functions were used. The results of the calculations together with the experimental data are shown in Fig. 24. The theoretical angular distributions reproduce the experimental distributions well for the normalization coefficient $N = 6$ in the case of the ^{12}C target and $N = 7$ for ^{16}O, corresponding to renormalization coefficients ~2.4–2.6 of the interaction strength. Similar results were obtained in other calculations

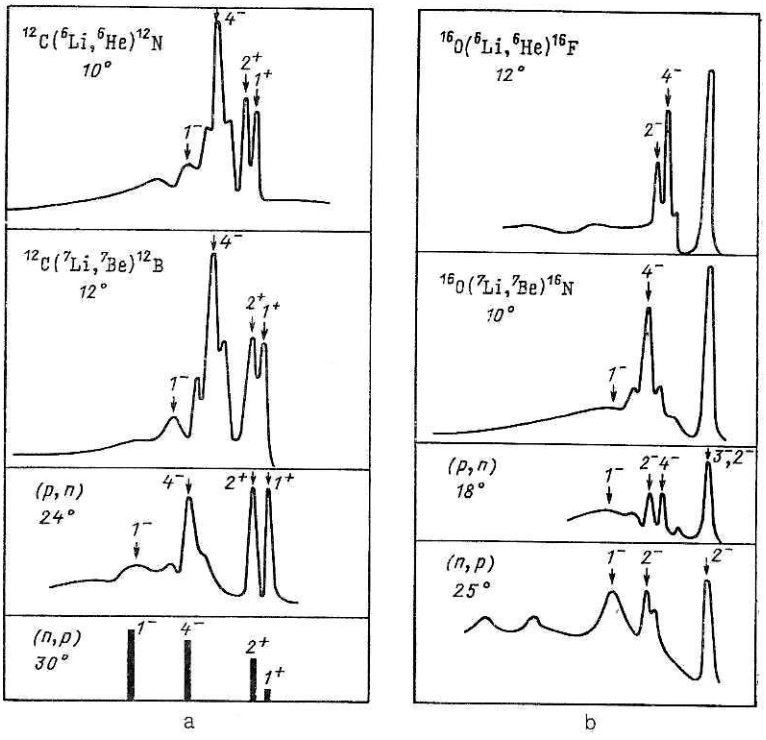

FIG. 23. Comparison of the energy spectra of the (^{6}Li, ^{6}He) reaction at $E_{^6Li} = 93$ MeV, (^{7}Li, ^{7}Be) reaction at $E_{^7Li} = 78$ MeV (p,n) reaction at $E_p = 99.1$ MeV (Ref 19), and (n,p) reaction at $E_n = 59.5$ MeV (Ref. 41), obtained at different angles on a ^{12}C target (a), and spectra of the same reactions obtained on a ^{16}O target at different angles (b). The energy spectrum from the $^{16}O(p,n)$ reaction at $E_p = 135.2$ MeV is taken from Ref. 23, and the one for the (n,p) reaction is from Ref. 41.

(^{7}Li, ^{7}Be) reaction with central forces.[6,72] In our opinion, the renormalization is probably due to the neglect in the calculations of the tensor component of the effective interaction. For in recent studies[73,73] it was shown that allowance for the tensor forces can decrease the renormalization coefficients by a factor of about 2. Thus, the contemporary data indicate that a direct one-step charge-exchange mechanism in which spin flip plays an important part is dominant in the (^{7}Li, ^{7}Be) reaction. However, if the part played by this mechanism is to be more accurately estimated it will be necessary to calculate two-step processes of successive one-nucleon transfer.

The (^{7}Li, ^{7}Be) reaction on intermediate and heavy nuclei

A comprehensive experiment in which the energy spectra of the (^{7}Li, ^{7}Be) reaction at beam energy 78 MeV were investigated on many target nuclei from ^{27}Al to ^{208}Pb was made in Ref. 75. The example of the spectrum on ^{27}Al is shown in Fig. 25. There are four strong groups of states with centers at excitation energies 2.0, 4.1, 6.2, and 9.3 MeV of the ^{27}Mg nucleus in a broad distribution with centroid at $E_x = 18$ MeV. For comparison, the figure also shows the spectrum of the (n, p) reaction measured at neutron energy 60 MeV.[42] The main difference between the two spectra is that for (^{7}Li, ^{7}Be) we can hardly observe the group of transitions at $E_x = 15$ MeV, which is dominant in the (n, p) reaction and corresponds to excitation of the electric dipole resonance of the ^{27}Al nucleus. The different selectivities in (n, p) and (^{7}Li, ^{7}Be) can be explained by the difference between the contributions of the spin-flip mechanism to these reactions.

The main reason for the appearance of a continuous spectrum in the (^{7}Li, ^{7}Be) reaction is probably either decay of an intermediate ^{8}Be nucleus into ^{7}Be + n [this mechanism was already discussed in the analysis of the spectra of the (^{6}Li, ^{6}He) reaction] or breakup of the ^{7}Li nucleus al-

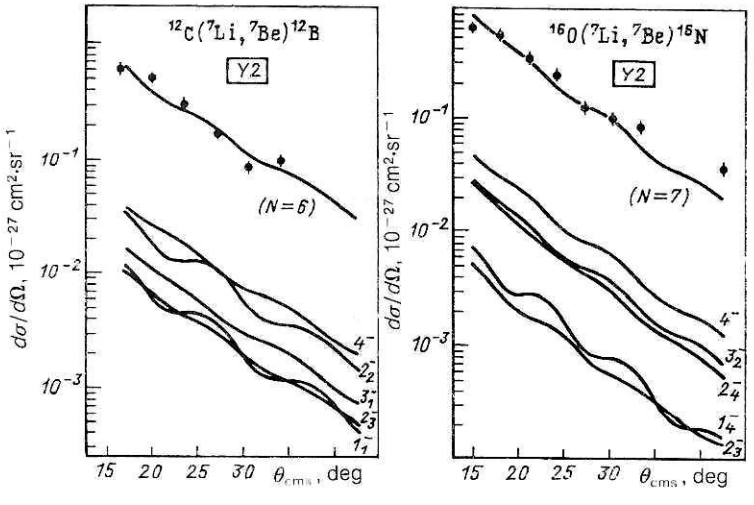

FIG. 24. Differential cross sections of the $^{12}C(^7Li, ^7Be)$ ^{12}B reaction with excitation of a group of states at $E_x = 4.5$ MeV and of the $^{16}O(^7Li, ^7Be)$ ^{16}N reaction with excitation of a group of states at $E_x = 6.2$ MeV. The curves are the partial and total theoretical cross sections. The total theoretical cross sections are multiplied by a factor $N = 6$ in the first case and $N = 7$ in the second.

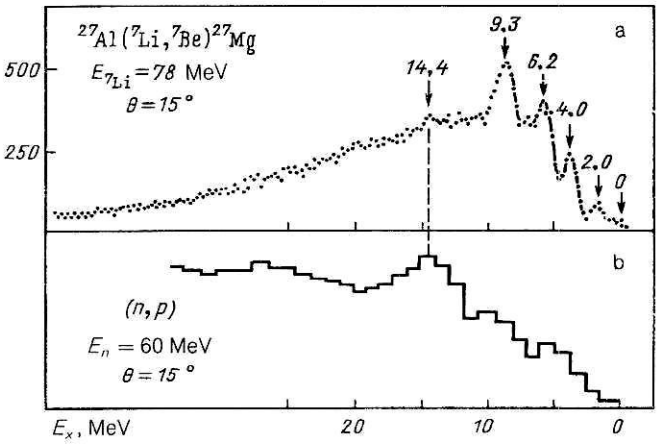

FIG. 25. Energy spectrum of ^{7}Be nuclei from the ^{27}Al(^{7}Li, ^{7}Be)^{27}Mg reaction, obtained at $E_{^{7}Li} = 78$ MeV at angle $\theta = 15°$ (a, Ref. 75); energy spectrum of protons from the ^{27}Al$(n, p)^{27}$Mg reaction, obtained at angle $\theta = 15°$ at $E_n = 60$ MeV (b, Ref. 42).

ready in the first step, $^{7}\text{Li} \rightarrow {}^{6}\text{Li} + n$, with subsequent pickup of a proton from the target nucleus. Results of investigation of the ^{27}Al(^{7}Li, ^{7}Be) reaction with lithium-ion energies from 100 to 180 MeV were recently published.[76] Examples of spectra taken from this study are shown in Fig. 26. It was found that the ^{27}Al(^{7}Li, ^{6}Li + X) continuous spectrum has a shape similar to the broad distribution observed in the (^{7}Li, ^{7}Be) case. This shows that of the two mechanisms mentioned above the second is the stronger. Comparison of the spectra of the (^{7}Li, ^{7}Be) reaction at 78 and 180 MeV shows that the growth of the $^{7}\text{Li} \rightarrow {}^{6}\text{Li} + n$ disintegration cross section with increasing beam energy may hinder investigation of the isovector resonances at high excitation energies.

Figure 27 shows the energy spectra of the (^{7}Li,^{7} Be) reaction for four nickel isotopes.[75] We observe the picture characteristic of the (^{7}Li, ^{7}Be) reaction on intermediate nuclei—a peak at excitation energies 4–5 MeV and broad distributions with centroids at $E_x \simeq 13$–16 MeV. With increasing neutron excess, on the transition from ^{58}Ni to ^{64}Ni, the peak at $E_x \sim 4$–5 MeV becomes much narrower, as we see in

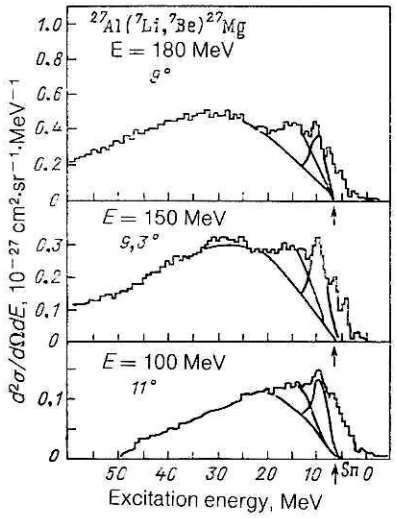

FIG. 26. Energy spectra of the ^{27}Al(^{7}Li, ^{7}Be) reaction, obtained for three different ^{7}Li energies.

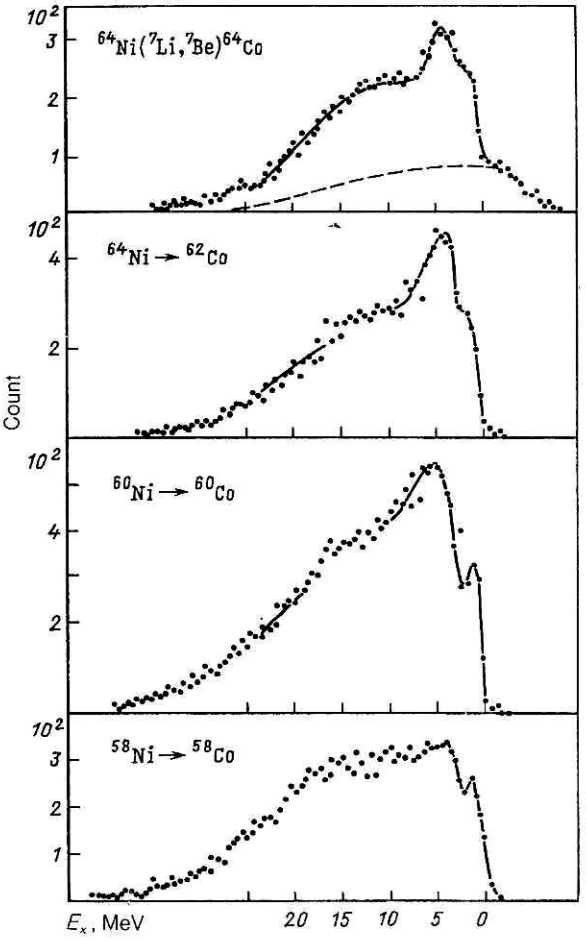

FIG. 27. Energy spectra of the (^{7}Li, ^{7}Be) reaction on nickel isotopes at $E_{^{7}Li} = 78$ MeV.

the figure, and the peak itself is more readily distinguished on the background of the broader distribution. Note that in the (n, p) reaction, in contrast to (^{7}Li, ^{7}Be), the main structure is found in the region of excitation energy 7–10 MeV (Ref. 41) and is associated with excitation of the $T_>$ component of the giant dipole resonance. Thus, the spectra of the (^{7}Li, ^{7}Be) reaction on the nickel isotopes differs strongly in its selectivity from the analogous spectra of the (n, p) reaction, just as we found for the case of ^{27}Al.

The complexity of the observed spectra of the (^{7}Li, ^{7}Be) reaction leaves us little hope of explaining their characteristic features by a limited number of multipolarities. Therefore, for more reliable conclusions, we need investigations that include a complete theoretical analysis of the differential cross sections with allowance for all states of particle–hole structure, as was done for the ^{90}Zr(^{6}Li, ^{6}He)^{90}Nb reaction discussed earlier. Investigations of such type were made in Ref. 77, in which the ^{90}Zr(^{7}Li, ^{7}Be)^{90}Y reaction at beam energy 78 MeV was studied. An example of the energy spectrum of the ^{7}Be nuclei from this reaction is shown in Fig. 28. On the background of a broad distribution we clearly observe peaks at excitation energies 4.6 and 1.5 MeV of ^{90}Y. The theoretical analysis was made in the framework of the one-step charge-exchange mechanism. The method used to calculate the cross sections is described above. The (^{90}Zr → ^{90}Y) transition densities which occur in the form-factor integrals were calculated on the basis of the theory of

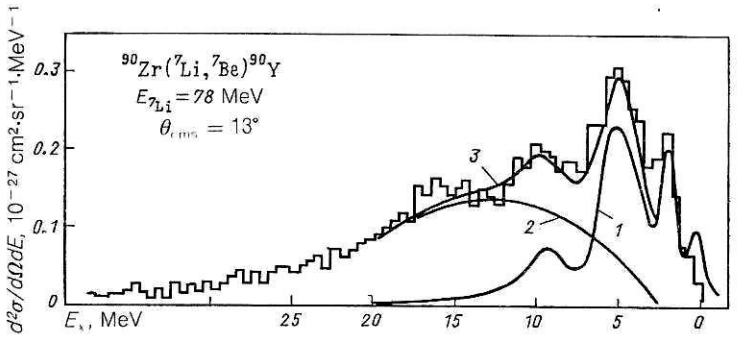

FIG. 28. Energy spectrum of the (^{7}Li, ^{7}Be) reaction on ^{90}Zr at $E_{^{7}Li} = 78$ MeV.

finite Fermi systems with allowance for the continuous spectrum and one-pion exchange.[67] The transition density of the $^{7}Li \to {}^{7}Be_0$ ($^{7}Be_1$) system was calculated with the cluster model. A restriction was made to central forces with radial dependence described by a sum of Yukawa potentials with the M3Y parametrization and the inclusion of an additional term to imitate exchange interaction.[6] The calculations took into account all particle–hole states of the ^{90}Y nucleus up to $J^{\pi} = 8^{-}$. The calculated spectrum is shown together with the corresponding "smearing" of the particle–hole transitions in Fig. 28 (curve *1*). The theoretical cross sections were multiplied by the coefficient 0.5, corresponding to a renormalization of the interaction by a factor 0.7. It can be seen that the theoretical distribution reproduces well the nature of the experimental spectrum at not too high excitation energies ($E_x < 6$ MeV), but with increasing excitation of the nucleus the difference in the absolute values of the cross sections increases strongly. The discrepancy between the theory and experiment in the region $E_x \geqslant 7$ MeV can be attributed to the contribution of two-step processes ($^{90}Zr + {}^{7}Li \to {}^{89}Y + {}^{8}Be^* \to {}^{89}Y + {}^{7}Be + n$ and $^{90}Zr + {}^{7}Li \to {}^{6}Li + n + {}^{90}Zr \to {}^{89}Y + {}^{7}Be + n$), which we have already considered for the case of ^{27}Al and which lead to continuous spectra (Fig. 28, curve *2*).

Figure 29 shows the partial differential cross sections for transitions of different multipolarities L. It can be seen that the nature of the spectra up to excitation energy ~ 3 MeV is basically determined by transitions with $L = 1$ and $L = 3$, while for $E_x > 7.0$ MeV transitions with $L = 4$ and $L = 6$ play the main part. As regards the region of the maximum of the experimental differential cross sections ($E_x = 4$–6 MeV), one can to almost equal degree speak of a contribution of all these multipolarities ($L = 1, 3, 4, 6$). The absence of $L = 0$ transitions is due to a blocking effect of the neutron excess.

6. COMPARISON WITH CHARGE-EXCHANGE REACTIONS ON HEAVY IONS

As we noted in the Introduction, in the charge-exchange reaction with lithium ions the contribution of the one-step mechanism must be greater than in reactions with other heavy ions if the comparison is made at the same energy per nucleon of the incident particle. We recall that this follows from the dependence of the reaction amplitude on the overlap integral of the wave functions of the incident and emitted particles [Eq. (1)]. Investigations of the reactions (^{6}Li, ^{6}He) and (^{7}Li, ^{7}Be), augmented by (^{12}C, ^{12}N), (^{12}C,

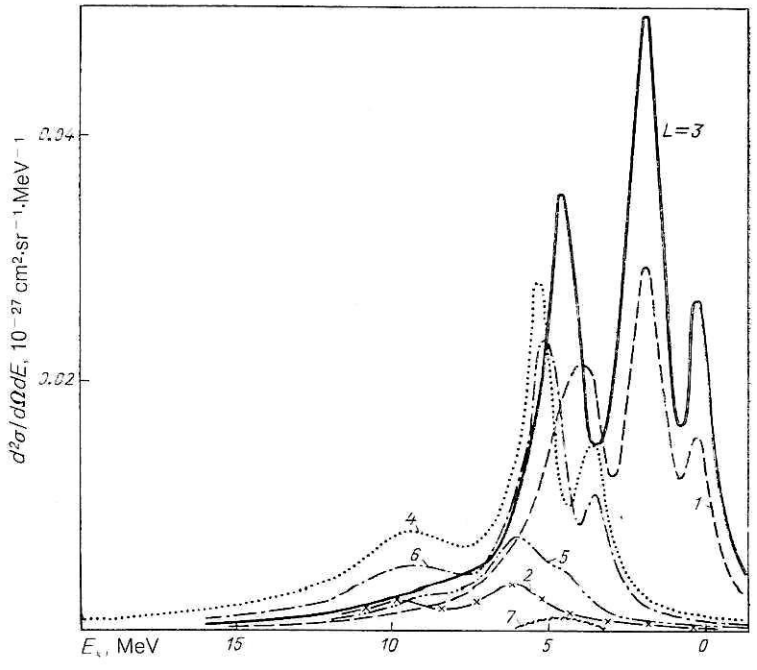

FIG. 29. Partial cross sections for the one-step charge-exchange mechanism in the $^{90}Zr(^{7}Li, ^{7}Be)^{90}Y$ reaction at beam energy 78 MeV.

TABLE IV. Strength of the spin–isospin interaction from different charge-exchange reactions.

Reaction	E, MeV	Type of interaction: Gauss, $a = 1.8$ F	Type of interaction: Yukawa, $a = 1.0$ F	Type of interaction: $M3Y$ *	Reference
(p, n)	20—50	7—21	11.7	0.43—0.55	[69, 78, 79]
(^{6}Li, ^{6}He)	34	—	14.2	—	[65]
			30		[11]
	93	10.7		1.3	[12, 66]
	210	—	14.4	—	[68]
(^{7}Li, ^{7}Be)	36	10	15.3	1.4—2.4	[6, 72]
	50	—	—	1.25—2.9	[73]
				0.75—0.9	[74]
	78	—	—	2.4—2.6	[13]
				0.7	[77]
(^{12}C, ^{12}B)	102	38—55	118—167	6.2—10	[80]
(^{12}C, ^{12}N)	420	—	32—300	—	[81]
(^{18}O, ^{18}F)	56	25	76	5.3	[82]

*The coefficients of the renormalization of the strength of the effective interaction are given here.

^{12}B), and (^{18}O, ^{18}F), confirm that the one-step mechanism is especially distinguished in reactions with lithium. Eloquent in this connection is Table IV, which gives the values of the phenomenological strength parameter of the spin–isospin interaction, $V_{\sigma\tau}$, obtained from analysis of various experimental data. The analysis was made under the assumption of a pure one-step process. It can be seen that in the (^{12}C, ^{12}N), (^{12}C, ^{12}B), and (^{18}O, ^{18}F) reactions the values of $V_{\sigma\tau}$ are, as a rule, appreciably greater than in the (^{6}Li, ^{6}He) and (^{7}Li, ^{7}Be) reactions. In turn, the values of $V_{\sigma\tau}$ for these last reactions agree with the values obtained in the (p, n) reaction. This indicates that in reactions with the heavy ions ^{12}C and ^{18}O a large proportion of the experimentally observed cross section is associated with a two-step process of successive one-step transfers.

The dependence of the cross sections of the one- and two-step processes on the beam energy for the (^{12}C, ^{12}N) case was estimated in Ref. 81. The case of successive transfers was calculated in accordance with the expression

$$\sigma_{\text{seq}} = \frac{A\sigma_1\sigma_2}{\sqrt{E}} \simeq \frac{A'\sigma_1^2}{\sqrt{E}}, \qquad (29)$$

where σ_1 and σ_2 are the cross sections for single-nucleon transfer in the first and second stages, calculated by the method of distorted waves, and A and A' are constants. The results of the calculations (Fig. 30) show that with increasing beam energy the cross section of the one-step process increases up to an energy of about 40 MeV per nucleon, while that of the two-step process decreases exponentially, so that only at $E \sim 50$ MeV/N do the two mechanisms become comparable.

An energy dependence of the cross sections of this kind is confirmed by more rigorous calculations[83–85] in which two-step transfers of a proton and a neutron were calculated with allowance for channel coupling. Figure 31, which is taken from Ref. 84, shows the energy dependence of the differential and total cross sections of the ^{12}C(^{12}C, ^{12}N)^{12}B reaction for transitions to the 1^+ ground state and to the excited states 2 ($E_x = 4.37$ MeV) and 4 ($E_x = 4.52$ MeV) of the ^{12}B nucleus. It can be seen that with increasing spin of the state the decrease of the cross section for the two-step process becomes less steep, and the region in which the one-step mechanism is dominant is shifted beyond the limit 100 MeV/nucleon.

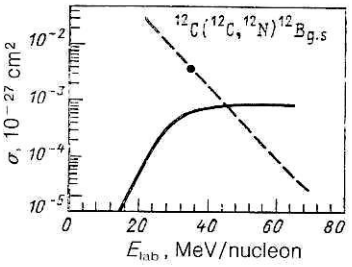

FIG. 30. Energy dependence of the cross sections of the ^{12}C(^{12}C, ^{12}N)^{12}B$_{g.s}$ reaction for the one- and two-step processes.

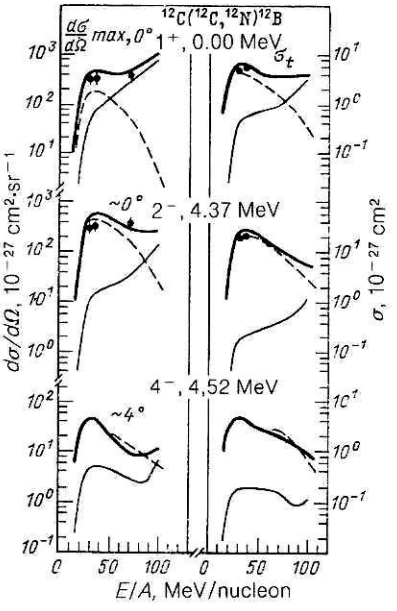

FIG. 31. Differential and total cross sections of the ^{12}C(^{12}C, ^{12}N)^{12}B reaction for transitions to the 1^+ ground state and the excited states 2^- ($E_x = 4.37$ MeV) and 4^- ($E_x = 4.52$ MeV) of the ^{12}B nucleus, as functions of the energy of the ^{12}C incident ion. The thin continuous curve represents the one-step charge-exchange mechanism, the broken curve represents the two-step process (calculation with allowance for channel coupling), and the heavy continuous curve represents their coherent sum.

7. THE (^{6}Li, ^{6}He) REACTION. APPLICATIONS

Search for effects of proximity to the threshold of π condensation

In the theory of finite Fermi systems it is shown that the energy of a pion in a nucleon medium, $\omega^2(k)$, has a minimum at a value of the momentum k near the Fermi momentum and may even vanish at a certain nucleon density.[86] In such a case, the nucleon matter would have an instability with respect to the pion field represented by a growth of the amplitude of the pion field with wave vector k_0, pions being spontaneously created. This phenomenon has become known as pion condensation. It is currently believed that a π condensate does not in fact exist in real nuclei, but it is very probable that the pionic degree of freedom is still strongly softened. Softening of the pionic mode must lead to effects that can be observed in a variety of nuclear processes. Such effects, which have been called precritical effects, are analyzed in detail in the review of Ref. 87. In particular, it is expected that proximity to the point of the π-condensate instability will influence the differential cross sections of reactions with excitation of anomalous-parity states.[87,88] According to the theoretical predictions, the greatest sensitivity must be manifested in the region of momentum transfers $q = (2\text{–}3)m_\pi$, where the pionic mode is maximally softened. In this region, a maxima may appear in the differential cross sections, its height being greater, the closer the nucleus is to the critical point.

The selective excitation of anomalous-parity states—states with pionic symmetry—makes it possible to use the (^{6}Li, ^{6}He) reaction to seek effects of proximity to the threshold of π condensation.

The behavior of the differential cross sections was investigated in Ref. 12 for a number of anomalous-parity levels excited in the ^{14}C(^{6}Li, ^{6}He)^{14}N reaction by 93-MeV ^{6}Li ions in the region of momentum transfers 0.6–2.3 F^{-1}. The angular distributions were calculated with transition densities obtained in the framework of the theory of finite Fermi systems on the basis of the approach described in Ref. 87. The effective NN interaction was a spin–isospin amplitude with explicit inclusion of one-pion exchange:

$$G = C_0\left[g'(\sigma_1\sigma_2) + g_{\pi}^{*}\frac{(\sigma_1 K)(\sigma_2 K)}{m_{\pi}^2 + k^2 + P_{\Delta}(k)}\right](\tau_1\tau_2). \qquad (30)$$

Here, g_π^* is the effective constant of the one-pion exchange, P_Δ is the polarization operator, which takes into account the contribution of the processes of virtual production of the Δ isobar and a nucleon hole, and k is the momentum transfer. The actual values of the constants that occur in the interaction are given in Refs. 12 and 87. The parameter g', which characterizes the short-range repulsion in the particle–hole channel, was regarded as a phenomenological constant and was determined by comparing theory with experiment. Its value is very important for conclusions about the proximity of real nuclei to the point of π condensation. The critical

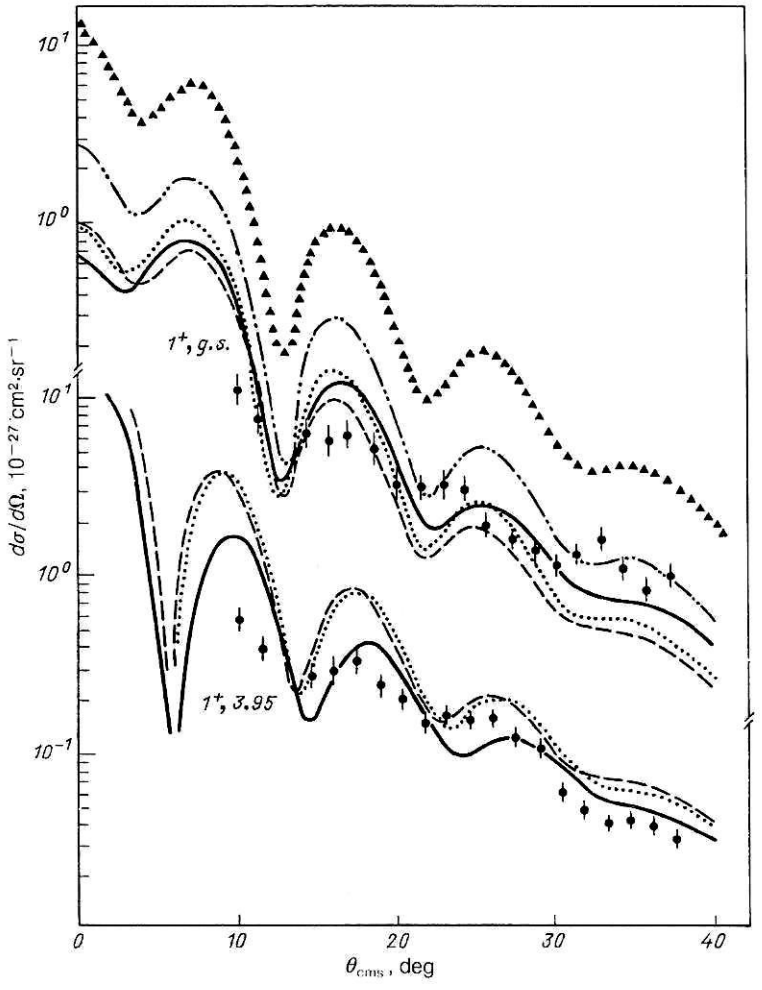

FIG. 32. Angular distributions of ^{6}He nuclei from the ^{12}C(^{6}Li, ^{6}He)^{14}N reaction for transitions to 1^+ states with $E_x = 0$ and 3.95 MeV at ^{6}Li ion energy 93 MeV. The continuous curves give the calculation with the transition densities for $g' = 1.1$, the dotted curves are for $g' = 0.7$, the chain curves are for $g' = 0.65$, and the broken curves are for $g' = 0.61$.

value of the parameter was estimated in Refs. 87 and 88 ($g'_{cr} = 0.605$ for 1^+ excitation). Thus, the proximity of the phase transition is characterized by the difference $g' - g'_{cr}$.

Figure 32 shows an example of comparison with experimental data of theoretical angular distributions for transitions to the 1^+ state of the ^{14}N nucleus, obtained for different values of the parameter g'.[12] It can be seen that for $g' \simeq 0.7$ a reasonable description of the angular distributions is still obtained. As g' is reduced to a value near the critical value, the absolute value of the cross section increases strongly in the complete range of angles. The predicted particular enhancement of the cross sections in the region of momentum transfers 1.4–2.1 F^{-1} (23–25°) is not observed. In Ref. 12, this is attributed to the insufficient sensitivity of the employed reaction to the putative effect, the reaction being of surface type. Indeed, calculations show that the transition density varies little on the surface of the nucleus for variation of g' up to about 0.7. In addition, distortions in the optical potential also lead to an additional and rather strong smoothing of the precritical effect. However, it should be noted that these facts do not exhaust all ways for further search for precritical effects in the (^{6}Li, ^{6}He) reaction. Experiments at high beam energies are extremely desirable, since they increase the sensitivity to the interior region of the nucleus.

Experimental determination of the form factor of the quasielastic process at short distances

Over many years great efforts have been made to obtain from experimental data, principally elastic scattering, unambiguous information about the potential of the internuclear interaction. The difficulty here is that the differential scattering cross section is strongly influenced only by a small number of partial waves corresponding to the strong-absorption range (R_a). Therefore, all potentials with a definite value near this range that correctly predict the phase shifts for a limited number of partial waves will give similar angular distributions. As a result, the interaction potential for $r \ll R_a$ remains undetermined, since the small partial waves that are sensitive to the interior region of the nucleus because of strong absorption make a very small contribution to the cross section.

Progress was achieved when the beam energy was increased, and the effect of nuclear rainbow scattering started to be observed in experiments. The characteristic features of the corresponding angular distributions can be explained by interference of waves scattered by the "near" and "far" edges of the nucleus. Under these conditions, the absorption was not so strong that it entirely washed out the effects of the refraction of waves with small angular momentum, and it thus became possible to probe the internuclear potential at distances appreciably less than the strong-absorption range.

It is natural to consider how much the refraction effects influence the other nuclear processes different from elastic scattering. In at least quasielastic processes, by which we mean interactions with a small change in the kinetic energy of the masses and charges of the colliding nuclei, we can expect to observe the same effects as in elastic scattering. It would then be possible (using knowledge of the potential determined unambiguously from the elastic scattering) to obtain important information about the mechanism of the quasielastic process and investigate the behavior of the form factors at short distances.

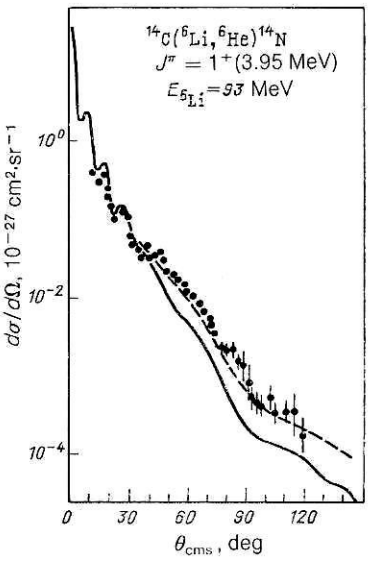

FIG. 33. Differential cross sections of the ^{14}C(^{6}Li, ^{6}He) ^{14}N reaction ($J^\pi = 1^+$, $E_x = 3.95$ MeV) at $E_{^6Li} = 93$ MeV. The continuous curve gives the calculation by the distorted-wave method with the theoretical form factor $F_{011}(r)$; the broken curve gives the calculation with an empirical form factor.

On the basis of this idea the ^{14}C(^{6}Li, ^{6}He) ^{14}N reaction with excitation of the 1^+ ($E_x = 3.95$ MeV) state of the ^{14}N nucleus was investigated[89] at beam energy 93 MeV in a wide range of angles up to 120°. The corresponding angular distribution is shown in Fig. 33. Data on the reaction were analyzed by the distorted-wave method in the framework of the one-step charge-exchange mechanism. Both central and tensor forces were taken into account. The experimental results and the calculations show that there is indeed a qualitative analogy between the charge-exchange reactions and elastic scattering. As in elastic scattering, the angular distribution of the reaction contains a diffraction structure, which is damped with increasing angle, and a monotonic decrease of the cross section at large angles. The observed diffraction structure can be explained by the interference of waves scattered by the near and far edges of the nucleus.

However, as can be seen from Fig. 33, the calculated cross section (continuous curve) for angles greater than 40° is more than 2 times smaller than the experimental cross section. There are two obvious ways to improve the agreement between the calculations and the experiment. The first is to give up the assumption that the potentials in the entrance and exit channels are identical. In Refs. 89 and 90 it was shown that a change, for example, of the imaginary part of the potential $W(^6\text{He})$, does not lead to a radical improvement of the agreement between theory and experiment in the range of angles 45–90°.

The second possibility is to modify the theoretical form factor. The empirical form factor was chosen in the form

$$F_{lsj}^{emp}(r) = F_{lsj}^{theor}(r)\left\{1 + \frac{4V\exp(-x)}{1+\exp(-x)}\right\},$$
$$x = (r - R)/\alpha. \qquad (31)$$

This corresponds to a slight raising of the theoretical form factor at distance R with intensity V and width α of the distribution.

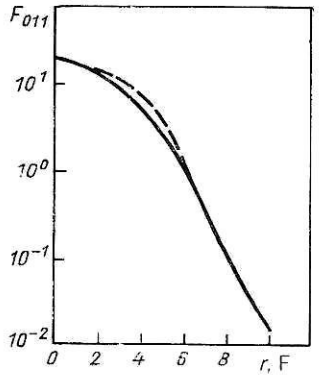

FIG. 34. Form factors of the ^{14}C(^{6}Li, ^{6}He)^{14}N reaction ($E_x = 3.95$ MeV, $J^\pi = 1^+$). The continuous curve is the theoretical form factor, and the broken curve is the empirical form factor calculated in accordance with Eq. (31).

Fairly good agreement can be achieved if we choose $R = 4.5$ F, $V = 0.7$, $\alpha = 0.6$ F. The broken line in Fig. 34 shows such a form factor. The cross section corresponding to it is shown by a similar curve in Fig. 33.

Thus, to describe the experimental data in a broad range of angles we must make a certain modification of the form factor, and this opens up a real possibility of obtaining from experiments information about the radial dependence of the form factors of direct reactions.

CONCLUSIONS

In this review, we have considered the results of investigations of charge-exchange reactions with lithium ions. Our main attention has been concentrated on experiments made recently at beam energies of more than 10 MeV/nucleon. The investigations have shown that the direct one-step charge-exchange mechanism with spin flip is dominant in the (^{6}Li, ^{6}He) reaction. Spin flip is distinguished in the (^{6}Li, ^{6}He) reaction because of the selection rules and the structure of the ground states of the ^{6}Li (1^+) and ^{6}He (0^+) nuclei. The (^{6}Li, ^{6}He) reaction differs advantageously from (p, n), in which (incomplete) selectivity to spin–isospin excitations arises only as a result of dynamical enhancement when the beam energy is raised to 100 MeV or higher. In accordance with the established mechanism, the cross section of the (^{6}Li, ^{6}He) reaction for Gamow–Teller transitions is proportional to the Gamow–Teller strength and, therefore, is, for a suitable calibration, a measure of it.

In the review we have analyzed the results of investigation of the (^{6}Li, ^{6}He) reaction on ^{27}Al and ^{90}Ar. We have seen that the Gamow–Teller and spin-dipole transitions cannot explain the nature of the experimental spectra and that in the (^{6}Li, ^{6}He) reaction, particularly at excitation energies > 10 MeV, spin-flip transitions with $L = 3$–5 play the main part. Thus, the (^{6}Li, ^{6}He) reaction can be used as a means of investigating spin–isospin excitations of high multipolarity. But if we are interested in separating the Gamow–Teller and spin-dipole resonances, we must make investigations at small angles and at high beam energies. However, recent experiments to study the ^{90}Zr(^{6}Li, ^{6}He)^{90}Nb reaction[91,92] showed that a 200-MeV energy of the ^{6}Li ions is still insufficient.

As yet, the mechanism of the (^{7}Li, ^{7}Be) reaction has been studied much less. However, the already existing data, obtained mainly at a beam energy around 11 MeV/nucleon, indicate that in this reaction the direct one-step charge-exchange mechanism, in which spin flip also plays an important part, is dominant. The (^{7}Li, ^{7}Be) reaction, like (^{6}Li, ^{6}He), differs strongly from other reactions with heavy ions: (^{12}C, ^{12}N), (^{12}C, ^{12}B), and (^{18}O, ^{18}F), for which, at least up to an energy of 50 MeV/nucleon, the main contribution is made by a two-step mechanism with successive transfers of a neutron and a proton.

In the (^{7}Li,^{7} Be) reaction on intermediate and heavy nuclei we observe a universal nature of the spectra, which are broad distributions with a maximum at $E_x = 4$–5 MeV. Investigation of the (^{7}Li, ^{7}Be) reaction on ^{90}Zr shows that in the excitation spectrum of the ^{90}Y nucleus regions in which transitions with $L = 1$ and 3 ($E_x < 3$ MeV) and $L = 4$ and 6 ($E_x > 7$ MeV) play the main role can be identified. To increase the sensitivity to transitions with $E_x > 7$ MeV, it is necessary to increase the beam energy. But as the energy increases, so does the cross section of the process that proceeds through a stage with disintegration of the nucleus, ^{7}Li–^{6}Li + n, with formation of a continuous spectrum, and this may hinder the investigation at high excitation energies.

In the review we have considered applications of (^{6}Li, ^{6}He) reactions to the investigation of precritical effects and the behavior of the form factor at short distances. We have shown that in both cases it is desirable to make the measurements at high beam energies in order to increase the sensitivity to the interior region of the nucleus. We have also shown that in calculations of the differential cross sections the lower boundary of the region of sensitivity to the form factor lies, already at energy 93 MeV, at a distance appreciably less than the strong-absorption range.

We thank Yu. A. Glukhov, S. A. Goncharov, A. S. Dem'yanov, N. I. Pyatov, and S. A. Fayans for collaboration in a number of studies discussed in this review and for discussions with them.

[1]J. D. Anderson and C. Wong, Phys. Rev. Lett. **7**, 250 (1961).
[2]D. E. Bainum, J. Rapaport, C. D. Goodman *et al.*, Phys. Rev. Lett. **44**, 1751 (1980).
[3]C. Gaarde, Nucl. Phys. **A396**, 127 (1983).
[4]V. I. Chuev, V. V. Davidov, V. I. Manko *et al.*, Phys. Lett. **31B**, 624 (1970).
[5]V. I. Chuev, V. V. Davidov, B. G. Novatsky *et al.*, J. Phys. (Paris) **32**, 6, 167 (1971).
[6]M. E. Williams-Norton, F. Petrovich, K. W. Kemper *et al.*, Nucl. Phys. **A313**, 477 (1979).
[7]F. Petrovich and D. Stanley, Nucl. Phys. **A275**, 487 (1977).
[8]F. A. Gareev, S. A. Goncharov, S. N. Ershov *et al.*, Yad. Fiz. **38**, 73 (1983) [Sov. J. Nucl. Phys. **38**, 41 (1983)].
[9]J. Bang and C. Gignoux, Nucl. Phys. **A313**, 119 (1979).
[10]V. I. Kukulin, V. M. Krasnopol'skiĭ, M. A. Miselkhi, and V. T. Voronchev, Yad. Fiz. **34**, 21 (1981) [Sov. J. Nucl. Phys. **34**, 11 (1981)].
[11]W. R. Wharton and P. T. Debevec, Phys. Rev. C **11**, 1963 (1975); W. R. Wharton, C. D. Goodman, and D. C. Hensley, Phys. Rev. C **22**, 1138 (1980).
[12]D. V. Aleksandrov, J. Bang, I. N. Borzov *et al.*, Nucl. Phys. **A436**, 338 (1985).
[13]J. Bang, F. A. Gareev, S. A. Goncharov, and G. S. Kasacha, Nucl. Phys. **A429**, 330 (1984).
[14]A. Laverne and C. Gignoux, Nucl. Phys. **A203**, 597 (1973).
[15]V. I. Kukulin *et al.*, Nucl. Phys. **A245**, 429 (1975).
[16]T. N. Taddeucci, C. A. Goulding, T. A. Carey *et al.*, Nucl. Phys. **A469**, 125 (1987).
[17]C. D. Goodman, C. A. Goulding, H. B. Greenfield *et al.*, Phys. Rev. Lett. **44**, 1755 (1980).
[18]D. G. Horen, C. D. Goodman, C. C. Foster *et al.*, Phys. Lett. **95B**, 27 (1980).

[19]J. N. Knudsen, B. D. Anderson, P. C. Tandy *et al.*, Phys. Rev. C **22**, 1826 (1980).
[20]T. N. Taddeucci, J. Rapaport, D. E. Bainum *et al.*, Phys. Rev. C **25**, 1094 (1981).
[21]J. Rapaport, T. Taddeucci, C. Gaarde *et al.*, Phys. Rev. C **24**, 335 (1981).
[22]C. D. Goodman, C. C. Foster, D. E. Bainum *et al* Phys. Lett. **107B**, 406 (1981).
[23]A. Fazely, B. D. Anderson, M. Ahmad *et al.*, Phys. Rev. C **25**, 1760 (1982).
J. Rapaport, T. Taddeucci, T. P. Welch *et al.*, Phys. Lett. **119B**, 61 (1982).
[25]B. D. Anderson, A. Fazely, R. J. McCarthy *et al.*, Phys. Rev. C **27**, 1387 (1983).
[26]C. Gaarde, J. Rapaport, T. N. Taddeucci *et al.*, Nucl. Phys. **A369**, 258 (1981).
[27]C. Gaarde, Phys. Scr. **5**, 55 (1983).
[28]J. Rapaport, Can. J. Phys. **65**, 574 (1987).
[29]A. Galonsky, J. P. Didelez, A. Djaloeis, and W. Oelert, Phys. Lett. **74B**, 176 (1978).
[30]O. Bousshid, H. Mashner, C. Alderlisten *et al.*, Phys. Rev. Lett. **45**, 980 (1980).
[31]S. Gopal, A. Djaloeis, J. Bojowald *et al.*, Phys. Rev. C **23**, 2459 (1981).
[32]D. Ovazza, A. Willis, M. Morlet *et al.*, Phys. Rev. C **18**, 2438 (1978).
[33]E. H. L. Aarts, R. K. Bhowmik, R. J. Meijer, and S. Y. Van der Werf, Phys. Lett. **102B**, 307 (1981).
[34]S. L. Tabor, C. C. Chang, M. T. Collins *et al.*, Phys. Rev. C **25**, 1253 (1982).
[35]C. Ellegaard, Can. J. Phys. **65**, 600 (1987).
[36]C. Ellegaard, C. Gaarde, J. S. Larsen *et al.*, Phys. Lett. **154B**, 110 (1985).
[37]D. Contardo, M. Bedjidian, J. Y. Grossiord *et al.*, Phys. Lett. **168B**, 331 (1986).
[38]V. G. Ableev, G. G. Vorob'ev, S. M. Eliseev *et al.*, Pis'ma Zh. Eksp. Teor. Fiz. **40**, 35 (1984) [JETP Lett. 40, 63 (1984)].
[39]V. G. Ableev, Kh. Dimitrov, S. M. Eliseev *et al.*, Preprint R1-87-374 [in Russian], JINR, Dubna (1987).
[40]F. Ajzenberg-Selove, R. E. Brown, E. R. Flynn, and J. W. Sunier, Phys. Rev. C **31**, 777 (1985).
[41]F. P. Brady and G. A. Needham, in *The (p,n) Reaction and Nucleon–Nucleon Force* (Plenum Press, New York, 1980), p. 357; N. S. P. King and J. L. Ullman, *ibid.*, p. 372.
[42]F. P. Brady, N. S. P. King, M. W. McNaughton, and G. R. Satchler, Phys. Rev. Lett. **36**, 15 (1976).
[43]F. P. Brady, C. M. Castaneda, G. A. Needham *et al.*, Phys. Rev. Lett. **48**, 860 (1982).
[44]G. A. Needham, F. P. Brady, D. H. Fitzgerald *et al.*, Nucl. Phys. **A385**, 349 (1982).
[45]J. L. Ullman, F. P. Brady, C. M. Castaneda *et al.*, Nucl. Phys. **A427**, 493 (1984).
[46]K. P. Jackson, A. Celler, W. P. Alford *et al.*, Phys. Lett. **201B**, 25 (1988).
[47]S. Yen, B. M. Spicer, M. A. Moinester *et al.*, Phys. Lett. **206B**, 597 (1988).
[48]M. C. Vetterli, O. Hausser, W. P. Alford *et al.*, Phys. Rev. Lett. **59**, 439 (1987).
[49]S. Yen, Can. J. Phys. **65**, 595 (1987).
[50]D. A. Lind, Can. J. Phys. **65**, 637 (1987).
[51]H. Conde, S. Crona, A. Hakansson *et al.*, Can. J. Phys. **65**, 643 (1987).
[52]D. Pocanic, K. Wang, C. J. Martoff *et al.*, Can. J. Phys. **65**, 687 (1987).
[53]D. P. Stahel, R. Jahn, G. J. Wozniak, and J. Cerny, Phys. Rev. C **20**, 1680 (1979).
[54]K. B. Beard, J. Kasagi, E. Kashy *et al.*, Phys. Rev. C **26**, 720 (1982).
[55]T. Motobayashi, H. Sakaii, N. Matsuoka *et al.*, Phys. Rev. C **34**, 2365 (1986).
[56]H. H. Duhm, N. Ueta, W. Heinecke *et al.*, Phys. Lett. **38B**, 306 (1972).
[57]C. Gaarde, T. Kammuri, and E. Osterfeld, Nucl. Phys. **A222**, 579 (1974).
[58]H. H. Duhm, H. Hafner, R. Refordt *et al.*, Phys. Lett. **48B**, 1 (1974).
[59]W. R. Wharton and P. T. Debevec, Phys. Lett. **51B**, 451 (1974).
[60]C. Gaarde and T. Kamnuri, Nucl. Phys. **A221**, 238 (1974).
[61]W. R. Wharton, J. G. Cramer, J. R. Calarco, and K. G. Nair, Phys. Rev. C **9**, 156 (1974).
[62]C. D. Goodman, W. R. Wharton, and D. C. Hensley, Phys. Lett. **64B**, 417 (1976).
[63]R. L. McGrath, D. F. Geesaman, L. L. Lee, and J. W. Noe, Phys. Rev. C **23**, 1060 (1981).
[64]A. Cunsolo, A. Foti, G. Imme *et al.*, Nucl. Phys. **A355**, 261 (1981).
[65]G. Ciangaru, R. L. McGrath, and F. E. Cecil, Nucl. Phys. **A380**, 147 (1982); Phys. Lett. **61B**, 25 (1976).
[66]A. S. Demyanova, S. A. Fayans, Yu. A. Glukhov *et al.*, Nucl. Phys. **A444**, 519 (1985).
[67]N. I. Pyatov and S. A. Fayans, Fiz. Elem. Chastits At. Yadra **14**, 953 (1983) [Sov. J. Part. Nucl. **14**, 401 (1983)].
[68]N. Anantaraman, J. S. Winfield, S. M. Austin *et al.*, Phys. Rev. Lett. **57**, 2375 (1986).
[69]S. M. Austin, in *The (p, n) Reaction and Nucleon–Nucleon Force* (Plenum Press, New York, 1980), p. 203.
[70]A. Guterman, G. Ciangaru, C. C. Chang *et al.*, Phys. Rev. C **27**, 1521 (1983).
[71]Yu. A. Glukhov, A. S. Dem'yanova, A. A. Ogloblin, and S. B. Sakuta, Yad. Fiz. **40**, 62 (1984) [Sov. J. Nucl. Phys. **40**, 41 (1984)].
[72]M. E. Williams-Norton, F. Petrovich, K. W. Kemper *et al.*, Nucl. Phys. **A275**, 509 (1975).
[73]J. Cook, K. W. Kemper, P. V. Drumm *et al.*, Phys. Rev. C **30**, 1538 (1984).
[74]A. C. Dodd *et al.*, J. Phys. G **11**, 1035 (1985).
[75]Yu. A. Glukhov, A. S. Dem'yanova, A. A. Ogloblin, and S. B. Sakuta, Yad. Fiz. **45**, 1236 (1987) [Sov. J. Nucl. Phys. **45**, 767 (1987)].
[76]S. Nakayama, T. Yamagata, K. Yuasa *et al.*, Phys. Rev. C **34**, 366 (1986).
[77]F. A. Gareev, Yu. A. Glukhov, S. A. Goncharov *et al.*, Yad. Fiz. **48**, 1217 (1988) [Sov. J. Nucl. Phys. **48**, 773 (1988)].
[78]T. Une, S. Tamaji, and H. Yoshida, Prog. Theor. Phys. **35**, 1010 (1966).
[79]F. Petrovich, R. H. Howell, C. H. Poppe *et al.*, Nucl. Phys. **A383**, 355 (1982).
[80]E. Etchegoyen, D. Sinclair, S. Liu *et al.*, Nucl. Phys. **A397**, 343 (1983).
[81]J. S. Winfield, N. Anantaraman, S. M. Austin *et al.*, Phys. Rev. C **33**, 1333 (1986).
[82]B. T. Kim, A. Greiner, M. A. G. Fernandes *et al.*, Phys. Rev. C **20**, 1396 (1979).
[83]H. Lenske, H. H. Wolter, and H. G. Bohlen, in *Proc. of the Intern. Nuclear Physics Conf.* (Harrogate, U.K., 1986), p. 197.
[84]H. G. Bohlen, H. Lenske, and H. H. Wolter, Jahresber. Hahn-Meitner-Institut (1987), p. 51.
[85]W. Von Oertzen, Preprint HMI-P 87/9 (1987).
[86]A. B. Migdal, *Theory of Finite Fermi Systems and Applications to Atomic Nuclei*, transl. of 1st Russ. ed. (Interscience, New York, 1967) [Russ. original, 2nd ed., Nauka, Moscow, 1983].
[87]I. N. Borzov, É. E. Sapershteĭn, S. V. Tolokonnikov, and S. A. Fayans, Fiz. Elem. Chastits At. Yadra **12**, 848 (1981) [Sov. J. Part. Nucl. **12**, 338 (1981)].
[88]W. Weise, in *Proc. of the International School on Nuclear Structure* (Alushta); Preprint D4-80-388 [in Russian], JINR, Dubna (1980), p. 231.
[89]A. S. Demyanova, A. A. Ogloblin, S. N. Ershov *et al.*, Nucl. Phys. **A482**, 383 (1988).
[90]A. S. Dem'yanova, E. Bang, F. A. Gareev *et al.*, Preprint R4-88-285 [in Russian], JINR, Dubna (1988).
[91]J. S. Winfield, N. Anantaraman, S. M. Austin *et al.*, Phys. Rev. C **35**, 1734 (1987).
[92]H. Wirth, R. Dietzel, W. Eyrich *et al.*, Phys. Lett. B (in press).

Translated by Julian B. Barbour